Understanding the Molecular Mechanisms that Contribute to Parkinson's Disease: Defining the Role of Ca^{2+} in TG2: α-synuclein Macromolecular Complex Assembly

by

James Washington

November 2018

Director of Thesis: Dr. Tonya N. Zeczycki

Major Department: Biochemistry and Molecular Biology

Transglutaminase 2 (TG2) is an allosteric enzyme ubiquitously expressed in human tissue. This versatile enzyme has both Ca^{2+} -dependent, transamidase and GTPase activities. TG2's Ca^{2+} -dependent transamidase activity is linked to many different diseases; most notably neurodegenerative diseases like Parkinson's. Initial Ca^{2+}-dependent, TG2 mediated post-translational modification of pathogenic proteins – including α-synuclein, tau, and β-amyloid— increases their aggregations potential. As the disease progresses, neuronal damage causes a loss of Ca^{2+} homeostasis (i.e. increasing intracellular Ca^{2+} concentrations) and further activation of TG2; these increased activities further facilitate the formation of pathogenic protein oligomers. As such, the exacerbated symptoms of neurodegenerative disease can, in part, be attributed to this destructive cycle. The allosteric mechanism by which Ca^{2+} controls TG2's transamidase activity is not fully understood. The currently accepted model posits that Ca^{2+} binding to TG2 *prior* to the protein substrate (i.e. α-synuclein) induces conformational changes necessary for substrate binding and catalytic turnover. However, our preliminary data, using α-synuclein as a model substrate, challenges this theory; our model indicates that Ca^{2+} binding occurs after enzyme-substrate complex formation. That is, Ca^{2+} activates the TG2: α-synuclein complex. In light of this data, we aim to answer the question "What role does Ca^{2+} have in activating of the

TG2: substrate complex?" We hypothesize that Ca^{2+} binding to the complex increases the stability of the enzyme: substrate complex, thereby increasing the rate of catalysis. Using Surface Plasmon Resonance (SPR), we have shown that the interactions between TG2 and α-synuclein do not adhere to a simple 1:1 binding model; as such, possible binding models for macromolecular complex formation are presented. We have also identified potential Ca^{2+}-binding regions on TG2 using multiple alignments. We expect our findings will be beneficial in developing an accurate model for TG2 activation, which can further be used to develop therapeutics that inhibit activity.

Understanding the Molecular Mechanisms that Contribute to Parkinson's Disease: Defining the Role of Ca^{2+} in TG2: α-synuclein Macromolecular Complex Assembly

A Thesis

Presented to

The Faculty of the Department of Biochemistry and Molecular Biology

East Carolina University

Brody School of Medicine

In Partial Fulfillment

of the Requirements for the Degree

Master of Science in Biomedical Sciences

James Washington

November 2018

Understanding the Molecular Mechanisms that Contribute to Parkinson's Disease: Defining Ca^{2+} Role in TG2: α-synuclein Macromolecular Complex Assembly

by

James Washington

APPROVED BY:

DIRECTOR OF
THESIS: _____
Dr. Tonya N. Zeczycki, PhD

COMMITTEE MEMBER: _____
Dr. Joseph Chalovich, PhD

COMMITTEE MEMBER: _____
Dr. Brian Shewchuk, PhD

COMMITTEE MEMBER: _____
Dr. Darrell Neufer, PhD

CHAIR OF THE DEPARTMENT
Biochemistry and Molecular Biology:_____
Dr. David Taylor, PhD (Interim)

DEAN OF THE
GRADUATE SCHOOL: _____
Paul J. Gemperline, PhD

ACKNOWLEDGEMENTS

I would like to thank the entire Zeczycki Lab for taking me in and providing numerous contributions to this project. I would also like to thank the East Carolina Diabetes and Obesity for allowing me to perform my research in their facility. I would also like my committee members, Dr. Joseph Chalovich, Dr. Brian Shewchuk, and Dr. Darrell Neufer for their support and guidance.

TABLE OF CONTENTS

LIST OF TABLES

LIST OF FIGURES

LIST OF ABBREVIATIONS

ATP	Adenosine Triphosphate (Page 7)
Ca^{2+}	Calcium (Page 2)
GTP	Guanine Triphosphate (Page 2)
SPR	Surface Plasmon Resonance (Page 11)
TG2	Transglutaminase 2 (Page 1)
WT	Wild Type (Page 12)
ZGG	Cbz-Gln-Gly (Page 9)

Section 1. BACKGROUND

1.1 **Neurodegenerative diseases are progressive and incurable.** As the population ages in America, the occurrence of neurodegenerative disease is becoming significant. Neurodegenerative disease is defined as the progressive loss and/or death of neuronal cells. This progressive loss of neuronal cells leads to the loss of both motor and memory function [25]. Alzheimer's and Parkinson's disease are the most prevalent of the neurological disorders. Alzheimer's disease affects roughly 16 million Americans and is currently the 6th leading cause of death in the United States; eclipsing both breast and prostate cancer deaths combined [11]. Similarly, Parkinson's disease affects ~1 million Americans, with an average of 60,000 new cases diagnosed each year [6]. As a whole, neurodegenerative diseases cost the nation 277 billion dollars; and this figure is expected to increase in the upcoming years. Currently, there is no cure for these diseases as most medicines only reduce the severity of the symptoms [24].

1.2 **The Ca^{2+}- dependent transamidase activity of transglutaminase 2 (TG2) leads to α-synuclein oligomerization and aggregation in the diseased brain.** A hallmark characteristic of both Alzheimer's and Parkinson's disease is the formation of both toxic protein oligomers and plaques in the diseased brain; the toxic protein oligomers and aggregates of α-synuclein and tau proteins are the underlying cause of neuronal death. α-Synuclein and tau are intrinsically disordered proteins which can form protofibrils, higher-order protein oligomers, and protein aggregates that induce disruption of cellular homeostasis [15-16]. There are numerous factors which trigger the formation of these protofibrils and oligomers, including the Ca^{2+}-dependent, post-translational modification by transglutaminase 2 (TG2). TG2 post-translationally modifies

both α-synuclein and tau proteins; these modifications result in proteins that are more prone to oligomerize and aggregate. [15-16].

Oligomerization of the pathogenic proteins leads to the formation of protein polymers that causes damage to the neuronal cells [15-16,18,30-31]. The TG2-mediated modification of these proteins can lead to the further damage of neurons, eventually ending in cell death. This pathway is illustrated in Figure 1. Damaged cells are also known to contain low levels of GTP and high levels of Ca^{2+}. This, along with oxidative damage, further promotes Ca^{2+}-dependent TG2 transamidase activity [15-16,18,30-31]. For example, in Parkinson's disease α-synuclein fibrils are key in the onset of the disease, as they are most abundant in intraneuronal Lewy bodies [15-16,39] (Figure 2). Studies have shown that TG2 catalyzes the formation of high molecular weight aggregates of α-synuclein which are characterized by protease resistant isopeptide bonds. It should be noted that α-synuclein can aggregate in the absence of TG2, with the potential for products to progress into fibrils [15-16,39]. Damaged neurons show increased Ca^{2+} levels and oxidative stress, both of which increase the Ca^{2+}- dependent activity, ultimately leading to increased oligomerization, protein aggregation, and eventually, neuronal death (Figure 1) [15-16,18,30-31]. However, the TG2-mediated post-translational modification and subsequent aggregation of modified α-synuclein represents a major oligomerization/aggregation pathway in both Parkinson's and Alzheimer's disease.

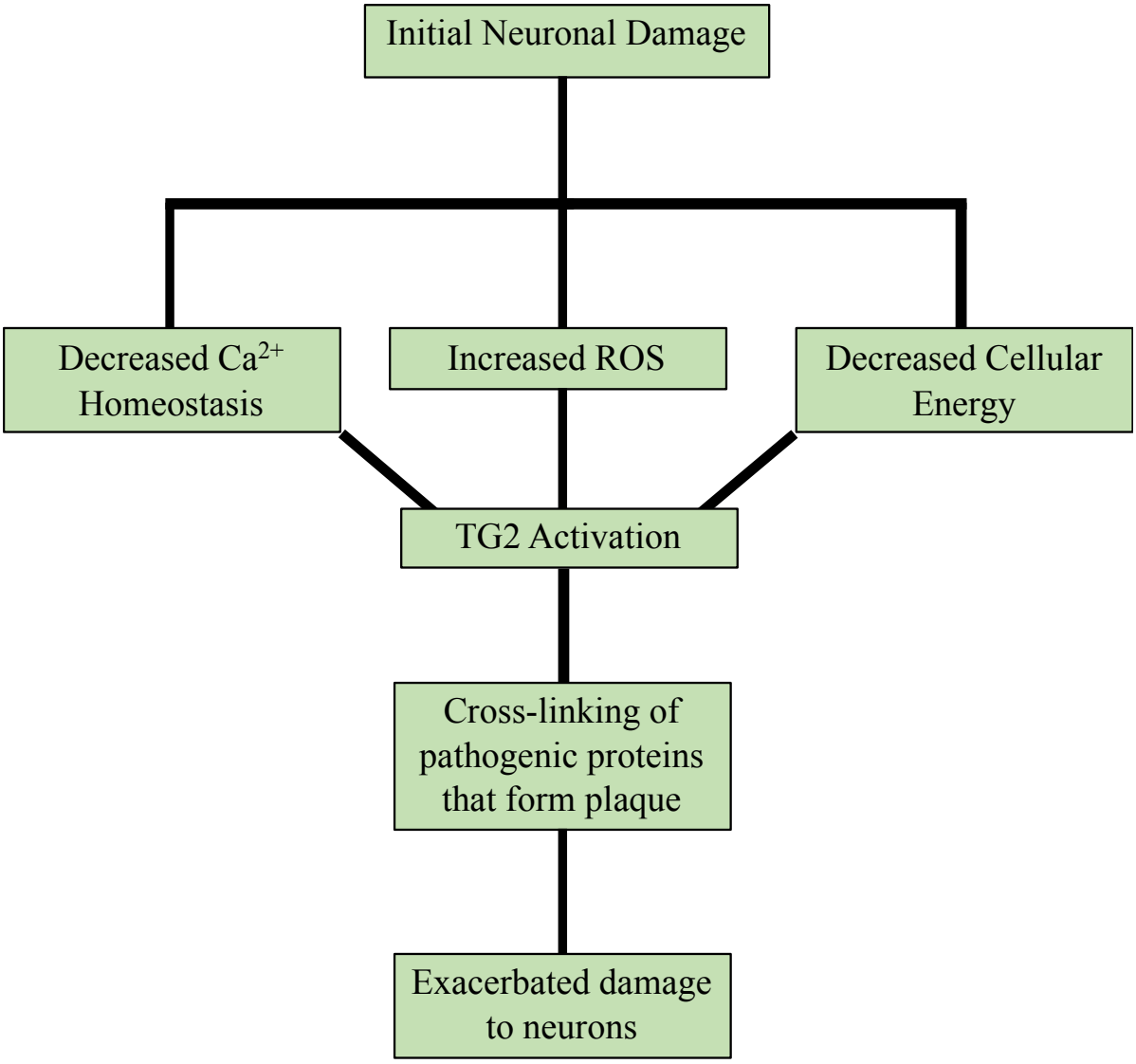

Figure 1: **TG2 activation in damaged neurons**. TG2 Ca^{2+}-dependent activity becomes uncontrolled due increased Ca^{2+} and oxidative stress induced by initial neuronal damage in the brain.

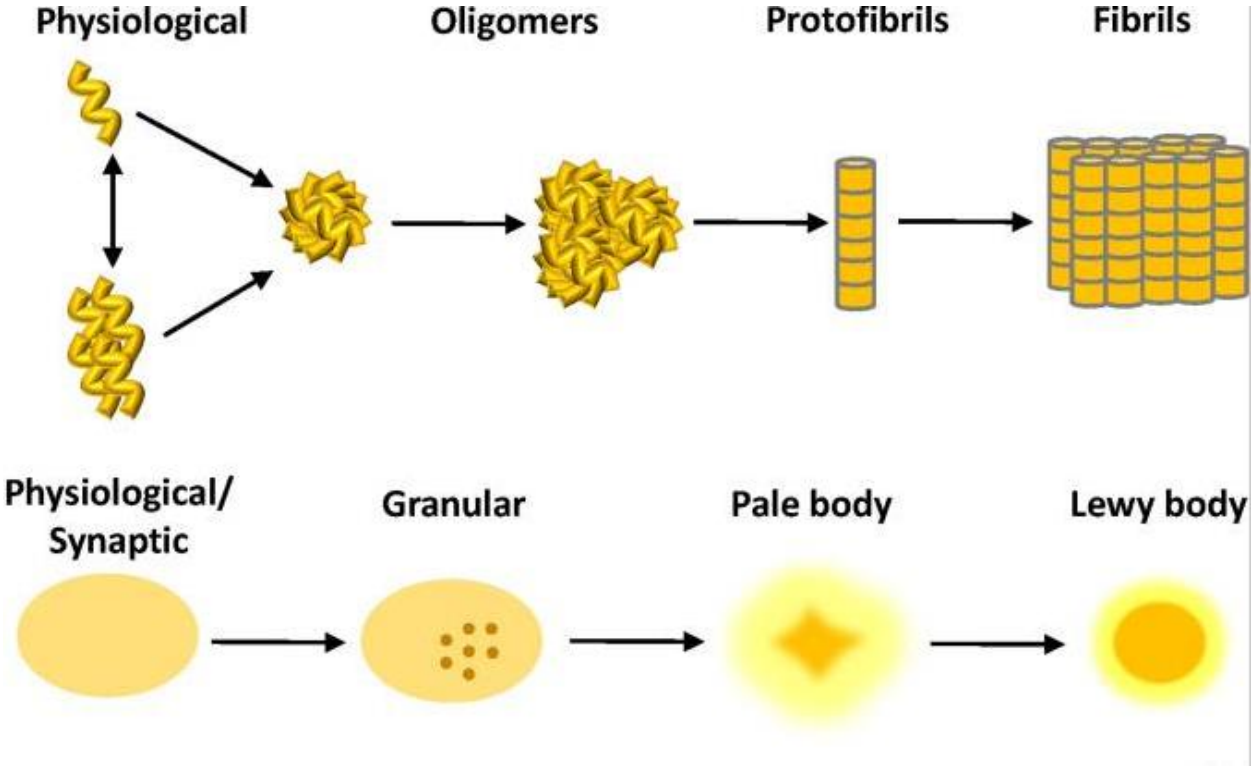

Figure 2: **α-Synuclein oligomerization pathway leads to formation of Lewy bodies**. Aggregation of α-synuclein is first observed in the form of granular deposits. From here, the deposits have the chance of progressing into Lewy bodies, which are pathognomonic to Parkinson's disease [2].

1.3 **TG2's Ca^{2+}- dependent activity proceeds through mechanism common to all members in the super family.** TG2 performs post-translational modifications of proteins via an initial deamidation and subsequent transamidation at specific reactive Gln residue. In these reactions, a strictly conserved, nucleophilic cysteine residue (Cys277 in *homo sapiens* and *mouse TG2*) nucleophilically attacks the γ- carbon of the peptide bound, glutamine side chain of a reactive Gln residue [16,17] (Figure 3). The result of these first steps of catalysis is the formation of a thioester acyl-enzyme intermediate concurrent with ammonia release. Water or a primary amine can subsequently perform a nucleophilic attack on the thioester bond. Attack by a water molecule results in deamidation of the Gln residue (i.e. Gln to Glu; Figure 4A). Attack with a

primary amine results in posttranslational modifications (Figure 4B). Although there has been speculation about what reaction is preferred, it is not fully understood which activity is favored. The site of transamidation activity consists of a catalytic triad: Cys277, His335, and Asp358 [16-17,27]. The Cys277 has been shown to be pivotal for transamidation activity. Two tryptophan residues (Trp241 and Trp332) form a catalytic tunnel which further stabilize the thioester intermediate during catalysis [16-17,27]. The two residues can be viewed as a "drawbridge" for substrate binding.

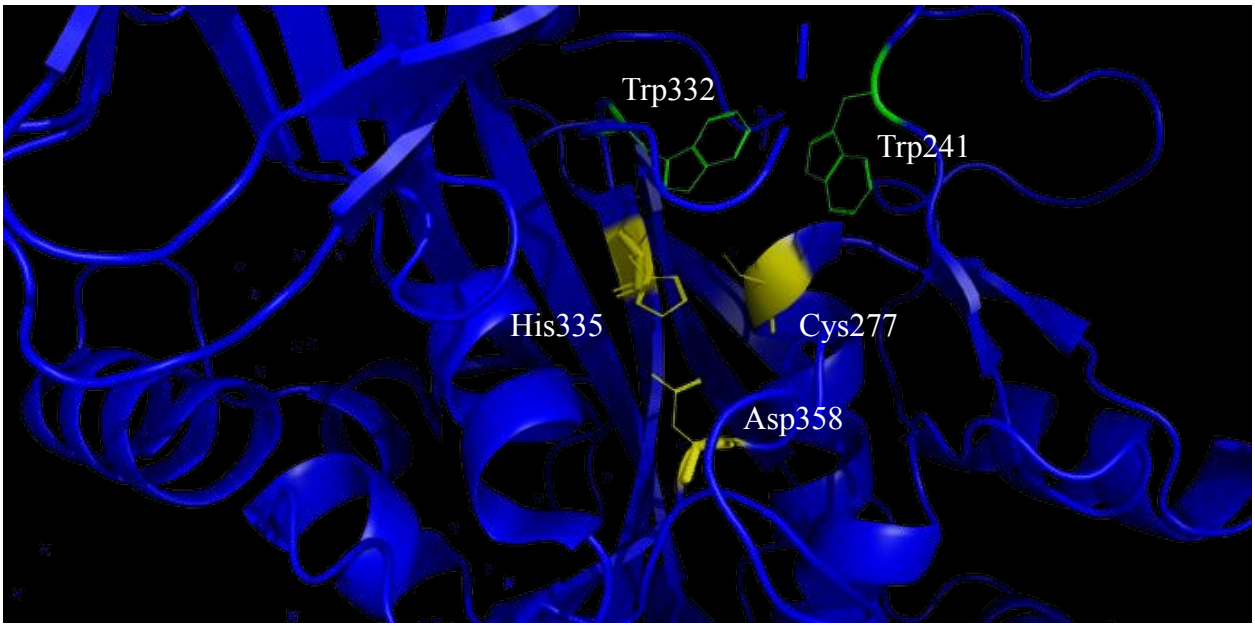

Figure 3: **The catalytic triad is the center for TG2 Ca^{2+}-dependent activity**. The catalytic triad (pictured in yellow) consists of Cys277, His335, and Asp358. Substrates must form a thioester linkage with Cys in order to initiate binding. Trp332 and Trp 241 act as a drawbridge for binding substrates.

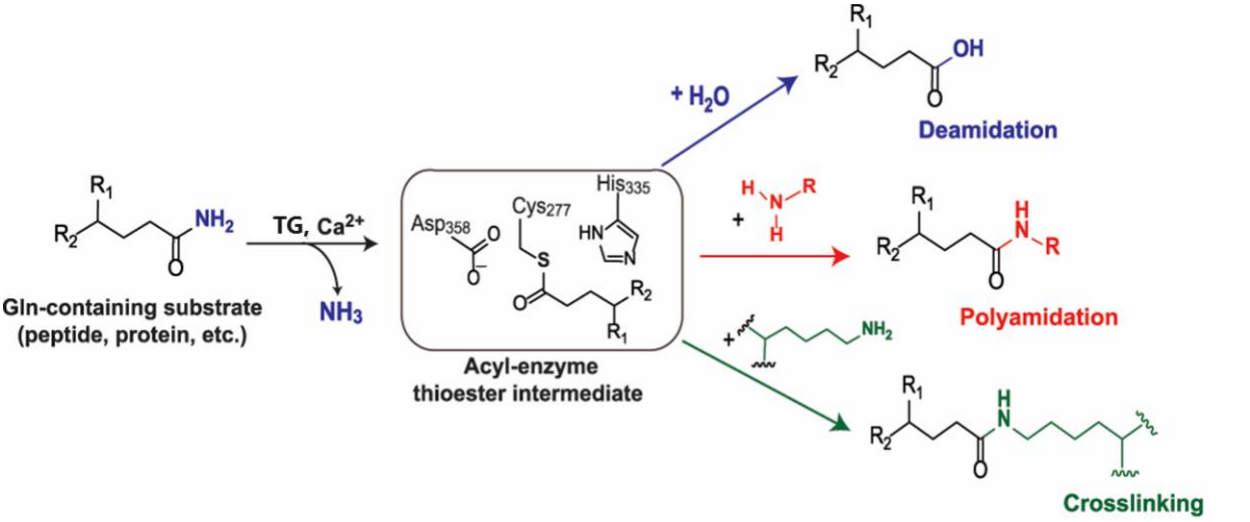

Figure 4: **Multiple pathways of transamidation.** After forming the acyl-enzyme intermediate, TG2 can (A) react with water to produce a glutamate residue, (B) react with a primary amine, or (C) react with the ε-group of a lysine resulting in a crosslinked protein.

1.4 **Even though the Ca^{2+}- dependent transamidase activity of TG2 in different pathways has been well documented, the allosteric mechanisms governing TG2's activity remain undefined.** Understanding how TG2 is regulated is important in order to comprehend both the biological and pathological activities of TG2. TG2 possesses numerous catalytic activities; most importantly the Ca^{2+} -dependent transamidase and Ca^{2+}-independent, GTPase activities [10,12,16-17,27, 28-29,32]. Studies have shown that TG2 is the α-subunit of a G Protein in different signaling pathways [12,16-17,20,27]. TG2 is further known to exhibit Ser/Thr kinase and protein disulfide isomerase (PDI) activities [16-17,29]. The Ca^{2+}-dependent and GTPase activities are mutually exclusive and reciprocally regulated such that Ca^{2+} inhibits GTPase activity and vice versa.

In the current model of TG2 regulation, the global conformation of TG2 is proposed to be directly related to these competing activities [20,27]. TG2 consists of four major domains: a N-terminal β-Sandwich, catalytic core, and two C-terminal β-barrels (Figure 5). TG2 with nucleotides bound such as GTP and ATP adopt a "closed" conformation supported by x-ray crystallography structures [20]. In this conformation, the C-terminal β-barrels fold over the catalytic core, potentially inhibiting any potential substrates from binding and concurrently forming a nucleotide binding site [20]. In contrast, TG2 is proposed to adopt an extended, or "open" conformation, allowing full access to the active site tunnel, thus supporting transamidation activity. In this conformation, the C-terminal β-barrels are stretched out, exposing the catalytic core [27].

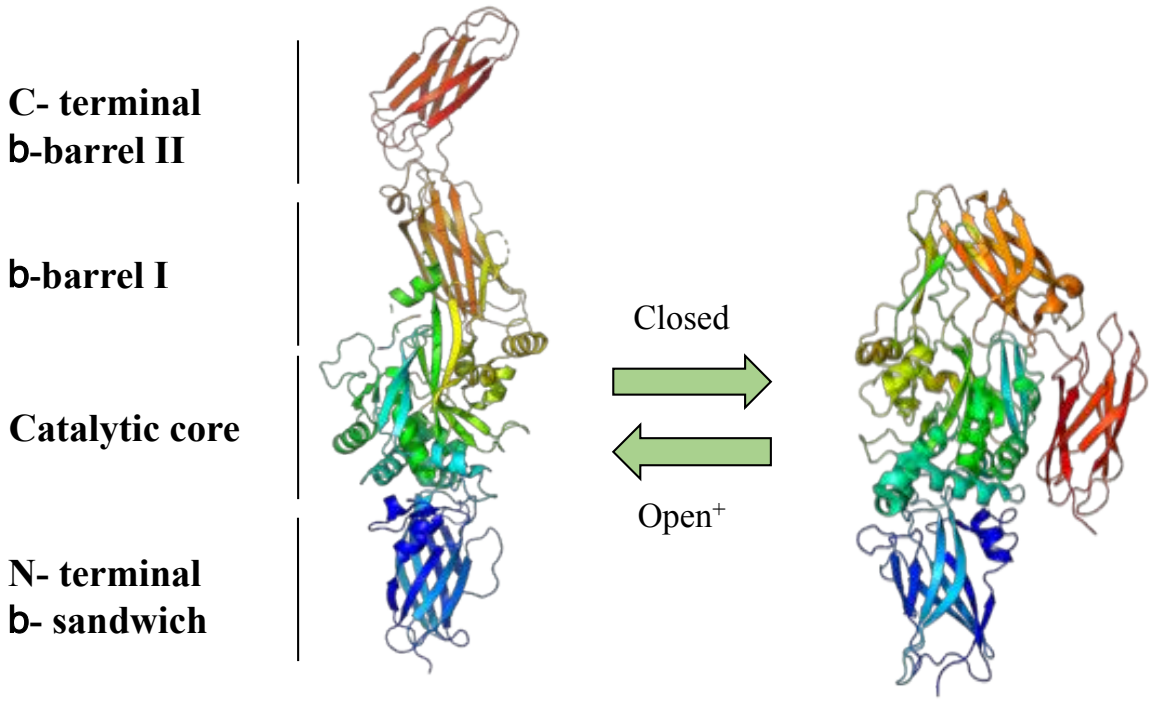

Figure 5: **TG2 undergoes a large conformational change upon GTP binding.** With Ca^{2+} independent activity, TG2 is seen folded in on itself, forming a "closed" conformation (PDB: 4PYG) [20]. Ca^{2+} dependent activity requires the enzyme to be in an "open" conformation (PDB: 2Q3Z) [27].

1.5 **The current accepted mechanism of TG2 activation of Ca^{2+} - dependent activity does not fully account for its *in vivo* activity.** The currently accepted allosteric mechanism governing the activation of TG2 suggests that Ca^{2+} binding to six sites on the enzyme promotes and stabilizes the "open" conformation and allows the substrate to bind [7]. Conversely, in the absence of Ca^{2+}, the enzyme is proposed to adopt a more closed structure, thus preventing transamidation activity. There are numerous studies, however, which suggests that this mechanism may not account for *in vivo* TG2 activity. Also, the crystal structure of the "open" or Ca^{2+}-dependent active conformation, does not contain any Ca^{2+}, even though the structure was obtained in the presence of 10 mM Ca^{2+}. The concentration is nearly 5-fold higher than the K_a

for Ca^{2+} determined with the non-natural substrate Cbz-Gln-Gly (ZGG). This structure did contain a covalently bound, peptide mimetic inhibitor, however, which might be responsible for the unique "open" structure.

Another potential issue is that most studies that have been done on TG2 use non-physiological substrates such as Cbz-Gln-Gly and uncommon substrates such as casein. These models could provide an inaccurate representation of how TG2 is being activated. For example, the K_m for Ca^{2+} determined with the artificial substrate Z-Gln-Gly was higher than the [Ca^{2+}] concentration in the cell. The apparent K_m for GTP is lower than what the [GTP] concentrations are in the cell. These data suggest, then, that TG2 is not active as a transamidase in the cell under normal physiological conditions; however, data show that TG2 is active as a transamidase in the cell when Ca^{2+} levels in nM range and GTP at μM ranges [36].

1.6 **In order to resolve the mechanism and advance our understanding of TG2's biological and pathological activities, the research here is focused on defining the role of Ca^{2+} in the formation of the TG2: α-synuclein complex.** In order to define the allosteric mechanism governing TG2 Ca^{2+}- dependent activity, we have undertaken substrate and Ca^{2+} binding and kinetic studies using α-synuclein as a model substrate. α-synuclein structure consist of three reactive Gln residues (Q79, Q99 and Q109) and two reactive Lys residues (K32, K80) [35]. We believe that using a physiological substrate will provide a more accurate activation mechanism. These sites are the targets of transamidation activity from TG2. The mechanism behind TG2's activation has been controversial because the current model suggests that TG2 can be activated by Ca^{2+} alone [7]. Preliminary data from our lab suggested that Ca^{2+} may be activating TG2 after substrate binding; as such ***we hypothesize that Ca^{2+} is activating the TG2: α-synuclein complex,***

rather than the enzyme itself, possibly by inducing catalytically relevant conformations in the ternary complex (Figure 6). In order to test this hypothesis and determine a functional role for Ca^{2+}, the work presented here aims to:

1. **Determine if α-synuclein binds to TG2 in the absence of Ca^{2+} and the effects of Ca^{2+} and electrostatics on the formation of the TG2: α-synuclein complex**
2. **Identify the role of Ca^{2+} in promoting or facilitating complex formation**
3. **Determine the location of unique Ca^{2+} binding sites**

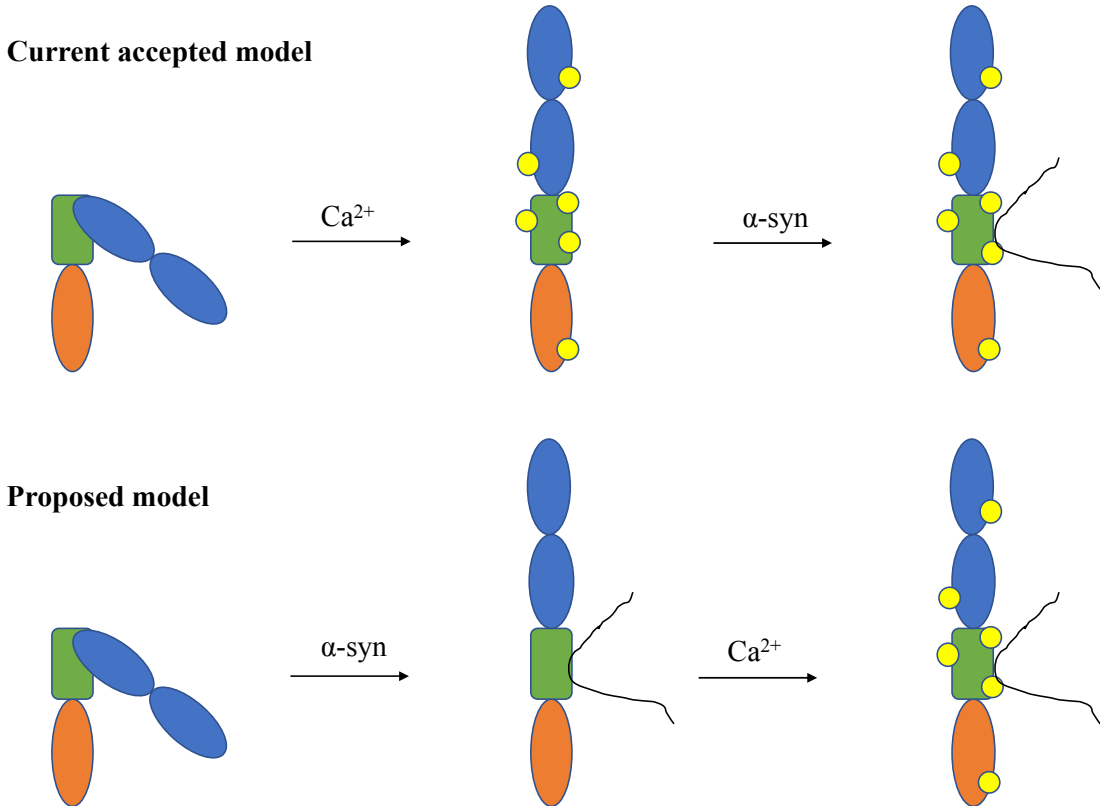

Figure 6: **The currently accepted model of activation of TG2 versus our predicted model.** Preliminary data confronts the idea that TG2 is activated by Ca^{2+} alone. We believe that there is a cooperative mechanism between the substrate and Ca^{2+} that activates TG2.

1.7 **If Ca^{2+} is not required for substrate binding, then it must play a role somewhere else in the mechanism.** For example, tightening the complex, conformational changes to promote catalysis or facilitating product release are all potential roles that Ca^{2+} provides. We used SPR, LRET/Tb^{3+} binding studies, and FURA-2 analysis to confirm our hypothesis. Bioinformatics was used to identify other possible Ca^{2+} binding sites. We determined how Ca^{2+} affects the activation of the TG2: substrate complex. Understanding how TG2 is activated will give us a better idea of why it affects patients suffering from neurodegenerative diseases. Furthermore, it will strengthen our foundational knowledge of the mechanism, which could lead to synthesis of effective TG2 inhibitors.

Section 2. DETERMINING the ROLE of Ca^{2+} IN ACTIVATING THE TG2 α-SYNUCLEIN COMPLEX

Introduction

The onset of neurodegenerative disease can be linked, in part, to catalytic activity between TG2 and α-synuclein [31,33]. Prior to modification, TG2 must first bind to α-synuclein and form the enzyme-substrate complex. Ca^{2+} plays a significant role in this mechanism as it is required for catalytic activity [31,33]. The currently accepted model of activation of TG2 shows that Ca^{2+} facilitates binding of α-synuclein by causing a conformational change in the enzyme's structure; however, our lab has evidence that this model may not be entirely accurate. In order to investigate the macromolecule assembly between the two proteins, we used Surface Plasmon Resonance (SPR). SPR uses evanescent waves to excite a gold film. The excitation creates plasmons that are sensitive to changes in molecular weight (Figure 7) [22,38]. We can use this to effectively study protein-protein interactions, and in this case TG2 complex formation [7]. In our studies we use a C277A mutant of TG2 that allows for complex formation but prevents catalytic turnover. This mutant has the same inherent binding affinities for both substrate and Ca^{2+} as the WT enzyme.

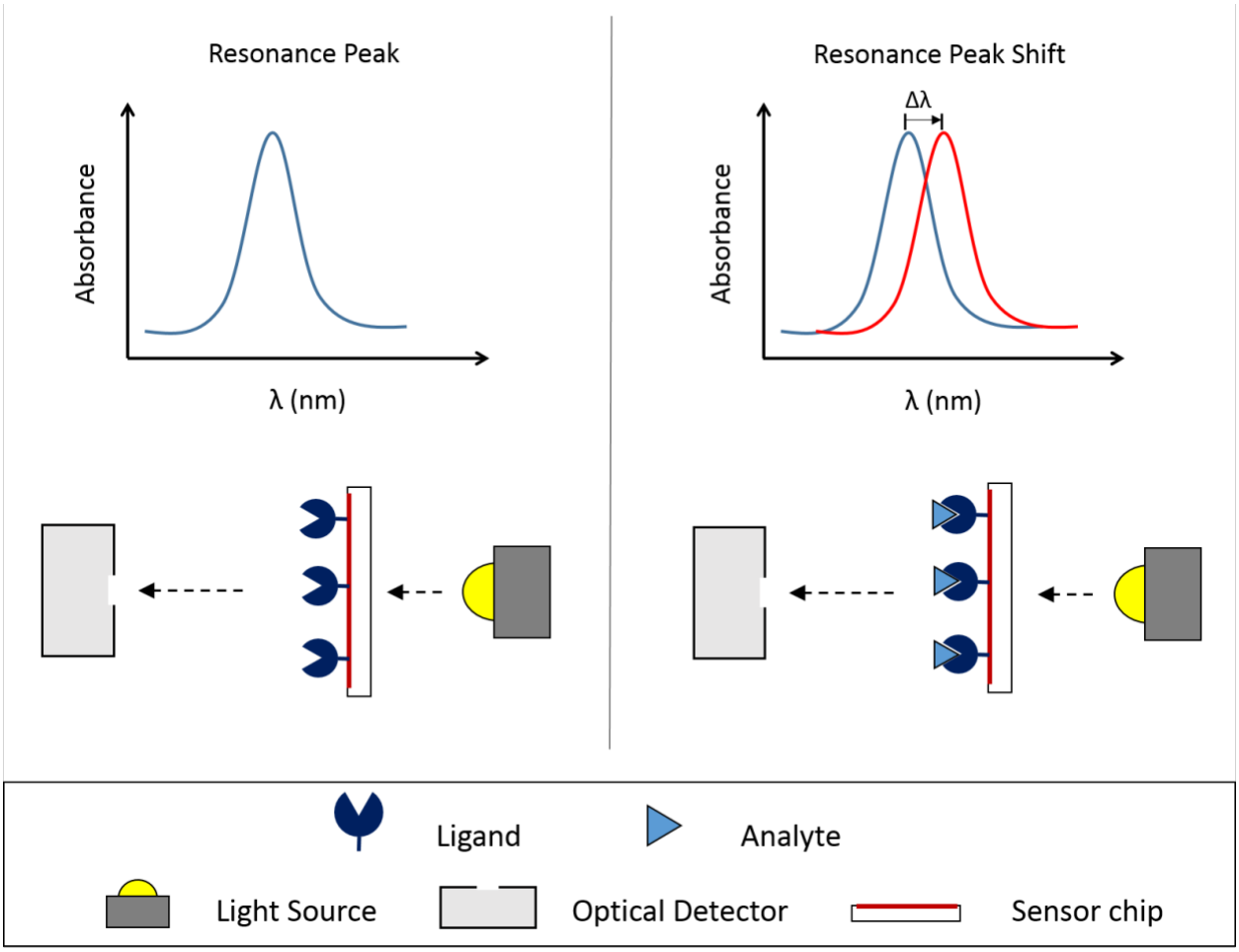

Figure 7: **Illustration of Surface Plasmon Resonance.** Depiction of how Surface Plasmon Resonance works [Nicoya]. Any conformations changes to the ligand will cause a shift in the resonance.

TG2 has many substrates however in this study we wanted to focus on three specific substrates. We start with TG2's interaction with α-synuclein which in this study, is being used as our model substrate. α-Synuclein structure is intrinsically disordered, which can potentially show a unique binding mechanism [23]. We also look at TG2's interaction with casein and Cbz-Gln-Gly. Casein's structure is known to contain order in its structure while Cbz-Gln-Gly is a non-physiological substrate primarily used for measuring transamidation assays. These structures are important because they are more popularly used in the field when studying TG2's catalytic activity. The majority of TG2's activation mechanisms that have been proposed have been based off of the use of these substrates [5,36].

SPR is further being used to determine if Ca^{2+} has a role in stabilizing the enzyme-substrate complex. In this study we started by focusing on complex formation in the absence of Ca^{2+}, as preliminary studies suggest that this is possible. We wanted to confirm this by investigating the interaction of TG2 and α-synuclein in a Ca^{2+}-free environment. Next, we investigated Ca^{2+} role regarding the stability of the complex i.e. if Ca^{2+} binding adds integrity to the TG2: α-synuclein complex. Ca^{2+} could also have an effect on the rate of complex formation. When α-synuclein first interacts with TG2, there could be a conformational change that allows Ca^{2+} to binding to available regions, which in term increase the speed at which the complex is formed. We propose that increasing Ca^{2+} does not have an effect on the association rate of α-synuclein, but however the increase of Ca^{2+} results in a tighter complex, decreasing dissociation rates.

Another point of interest is to study the effect of ionic strength on TG2. Ionic strength is important, as it can affect interactions between TG2 and α-synuclein [9,40]. For example, if

complex formation is driven by electrostatics, altering ionic strength can affect the affinity towards α-synuclein. Studying this affect could lead to a more complete understanding of TG2's activation mechanism.

Finally, we use FURA-2 to investigate equilibrium binding between TG2 and Ca^{2+} in the presence and absence of α-synuclein. FURA-2 is a high affinity fluorescent probe that can measure low Ca^{2+} levels in solution. By using an EGTA buffer system, we can control available Ca^{2+} and measure binding as the complex continues to form [28]. We seek to find the relationship between TG2 and Ca^{2+} as well as make assumptions about the enzyme: substrate complex.

Methods and Materials

Materials

The BCA assay kit, Ni^{+}- NTA resin, and Tris-HCl buffer was purchased from Thermosphere Scientific (Waltham, MA). Glycerol was purchased from Research Products International (RPI; Mt. Prospect, IL). FURA-2 potassium salt was purchased from Enzo Lifesciences (Farmingdale, NY). All other chemicals were purchased from VWR International (Radnor, PA) and of the highest purity available.

Overexpression of TG2 and α-synuclein

Electrocompetent BL21STAR(dE3) *E. Coli* were transformed with either the plasmid containing wild-type TG2 (pET-17b backbone) or α-synuclein (p-Receiver 01 backbone, Gencopia) and allowed to recover for 1 hour in 1 mL of SOC Media. ~25 µL of media was transferred to a Luria broth plate containing 35 mg/mL kanamycin (TG2) or 10 mg/mL ampicillin (α-synuclein) for plasmid maintenance and incubated for ~12 hours at 37 ºC. Individuals colonies were chosen at random and allowed to grow in 5 mL of Luria broth at 37 ºC containing the respective antibiotic. The 5 mL culture was used to inoculate 1 L of LB medium overnight with antibiotic (~12 hours of incubation time), which was later used to inoculate a 20 L carboy containing LB medium. The large-scale growths were carried out in a fermenter equipped with an air-inlet hose as well as a gas diffusion stone to provide bacteria with proper aeration. 0.75 g of kanamycin or 2.0 g of the ampicillin was added to the carboy as well as 1 mL of Antifoam 204 (Sigma Aldrich). ~10 mL of the overnight cells was added to the carboy and allowed to grow at a temperature of 37 ºC. This gave a starting optical density of roughly 0.010

A. Once an OD_{600} of ~0.6 – 0.7 A was reached, cells were immediately cooled to 20 ºC and 5.0 g of IPTG (final concentration 1 mM) was added to induce protein expression. Cells were allowed to further incubate for 18 hours. 10 mL of media was transferred to a separate container after incubation to test the cells for protein expression. Cells were harvested using a Sorvall LYNX 4000 Centrifuge (5000 rpm for 10 minutes) and flash-frozen in liquid nitrogen, yielding between 50 to 150 g of cell paste. The frozen cell pellets were stored at -80 ºC.

Purification of Wild-Type and Mutant Forms of TG2

Protein was purified using a combination of Ni^{2+}- affinity chromatography and Q-Sepharose ion exchange chromatography. ~20 g of cell paste was thawed in ~250 mL of lysis buffer (50 mM Na-Phosphate, pH 8.0, 300 mM NaCl) and ~200 µg/mL of lysozyme with stirring for ~15 minutes. Cells were then lysed by sonication using a Branson Digital Sonicator for 6 minutes (80% amplitude; pulse on: 59.9 seconds; pulse off: 30 seconds; max temp: 10 ºC). The lysate was clarified via centrifugation (10,000 rpm for 20 minutes using a Sorvall LYNX 4000 Centrifuge). The remaining supernatant was allowed to batch bind with ~10 mL of Ni^{+}-NTA Resin while rotating (2 hours; 4 ºC). Before being used for binding, the resin was pre-equilibrated with 5 column volumes of Milli-Q and 5 column volumes lysis buffer. After batch binding the resin was spun down at 4500 rpm for 15 minutes. The remaining supernatant was discarded and the resin was loaded onto a glass column and washed with 10 column volumes of wash buffer (50 mM Na-Phosphate pH 8.0, 300 mM NaCl, 10 mM imidazole;1.5 mL/min). TG2 was eluted with an elution buffer (50 mM Na-Phosphate pH 8.0, 300 mM NaCl, 750 mM imidazole) over a 300 mL linear gradient (1.5 mL/min). Fractions of interest were ran on a SDS-PAGE gel (5% stacking/9% resolving, 150 Volts, 1 hour) and those containing TG2 were

dialyzed overnight (2 X 1L; 20 mM Tris pH 7.2, 50 mM NaCl, 1 mM DTT, 1 mM EDTA) at 4 ºC.

Dialyzed proteins were loaded onto ~10 mL of Q-Sepharose™ Fast Flow resin at 1.5 mL/min. The resin was pre-equilibrated with 10 column volumes of Buffer A (20 mM Tris pH 7.2, 1 50 mM NaCl, 1 mM DTT, 1 mM EDTA). The loaded protein was washed with 10 column volumes of Buffer A and eluted with 150 mL linear gradient of Buffer B (20 mM Tris pH 7.2, 1M NaCl, 1mM DTT, 1 mM EDTA). Fractions of interest were analyzed SDS-PAGE (5% stacking/9% resolving; 150 Volts; 1 hour) and dialyzed overnight (2 X 1 L 20 mM MOPS pH 7.2, 150 mM NaCl, 1 mM DTT, 1 mM EDTA) at 4 ºC.

Purified protein was concentrated via centrifugation (4500 rpm; 15 minutes). A Vivaspin 20 centrifugal concentration tube (50 kDa MWCO; Sigma Aldrich) was used to concentrate to ~6 mg/mL. 10% glycerol was added dropwise, on ice, to the protein prior to flash-freezing and storage at -80 ºC. A BCA assay (Thermofisher) was performed to calculate the final protein concentration.

Purification of α-synuclein

Purification of α-synuclein follows the same initial Ni^{2+}- affinity chromatography protocol with a few changes. α-synuclein lysis buffer consisted of 20 mM Na- Phosphate (pH 8.0), 300 mM NaCl, and 1 mM PMSF. The wash buffer consisted of 20 mM Na- Phosphate (pH 8.0), 300 mM NaCl, and 10 mM imidazole. Elution buffer consisted of 20 mM Na- Phosphate (pH 8.0), 300 mM NaCl, and 750 mM imidazole. Two SDS-PAGE gels (5% stacking/12% resolving; 150 V; 1 hour) were ran to test for fractions of interest. Fractions containing protein were transferred to Spectra/Por Dialysis tubing (3-5 MWCO; Spectra) and dialyzed initially for

one hour, then overnight (2 X 1 L 20 mM Tris- HCl pH 7.2, 150 mM NaCl, 1 mM DTT, 1 mM EDTA) at 4 ºC. After dialysis the protein was concentrated using a Vivaspin 20 centrifugal concentration tube (3 kDa MWCO; Sigma Aldrich). α-synuclein was concentrated to about 0.8 mg/mL. Protein was aliquoted into small centrifuge tubes without addition of 10% glycerol. Protein was flash-frozen and stored at -80 ºC. A BCA assay was ran to confirm protein concentration.

Surface Plasmon Resonance (SPR) Experiments

SPR data was all recorded on an OpenSPR system (Nicoya Lifesciences). For all experiments 20 mM MOPS (pH 7.2), 150 mM NaCl, 1 mM DTT, and 0.005% Tween 20 was used for as a base running buffer. Depending on experimental conditions 1 mM EGTA and 10 nM-10 mM Ca^{2+} were also added to the running buffer. Purified TG2 or α-synuclein (200 µL; 50 µg/mL) was immobilized on a gold plated, -COOH functionalized chip according to manufactures instructions. TG2 was previously dialyzed overnight in a running buffer containing 10 mM EGTA. Amine Coupling Kit (Nicoya) was used to immobilize protein at a flow rate of 20 µL/min. After injection of protein, a blocking solution (200 µL) followed by regeneration solution (200 µL of 1 M NaCl) was allowed to run through the system (10 min). With α-synuclein on the chip, regeneration solutions consisted of 1M NaCl and 10 mM NaOH.

All experiments started with injections of small amounts of analyte to dictate concentration range (1nM – 15µM). Depending on dissociation efficiency, the chip was reconditioned with the regeneration solution at a pump speed of 50 µL/min for ~1 min then allowed to run for an additional 3 min before reverting back to 20 µL/min. Data obtained over a variety of chips to eliminate chip-to-chip variability.

Ca^{2+} Binding Studies using FURA-2 Fluorescent Probe

Ca^{2+} binding studies with FURA-2 were conducted using a Biotek Cytation5 Reader. Buffer A (100 mM MOPS pH 7.2, 750 mM NaCl, 50 mM EGTA) and Buffer B (100 mM MOPS pH 7.2, 750 mM NaCl, 50 mM EGTA, 50 mM $CaCl_2$) were used to control Ca^{2+} concentrations. A standard curve was also prepared for data analysis (ThermoFisher). Samples and standards were prepared in black Eppendorf tubes to protect from light. Prepared samples were allowed to incubate for 1 hour at room temperature. After incubation, 3 μM of FURA-2 probe was added to each tube and samples were aliquoted in triplicate to a black 96-well reading plate. The fluorescence of each sample was read immediately at 25 ºC. Samples were subjected to a constant excitation at 510 nm and the emission was measured from 300 nm to 600 nm.

Data Analysis

Surface Plasmon Resonance (SPR) Analysis

The amount of TG2 or ligand α-synuclein immobilized to each chip was calculated from the differences in the wavelength before and after addition. The ligand immobilization level, which varied with each chip and was used to determine the theoretical maximal signal response, R_{max}, using eqn (1)

$$R_{max}(pm) = \frac{analyte\ MW}{ligand\ MW} * ligand\ immobilization\ level\ (pm) \qquad \text{eqn 1}$$

where analyte MW and ligand MW are the molecular weights of the analyte and ligand, respectively. The ligand immobilization level was calculated from the change in wavelength before and after addition of ligand. SPR curves were generated by plotting arbitrary response units (RU) vs. time. Responses are derived directly from changes in wavelength. The SPR sensorgrams were reference corrected and blank injections were subtracted from the observed data. Sumerograms for individual experiments were fitted to either a 1:1 (Langmuir model, eqn 2) or 1:2 state binding model (eqn 3) [Biacore Lifesciences]. For a 1:1 interaction, data were globally fitted to the following differential eqn using Tracedrawer (v 1.8) using numerical integration:

$$\frac{dY}{dt} = (k_a * c - k_d) * Y \qquad \text{eqn 2}$$
$$Y(0) = 0, signal\ from\ saturated\ target = B_{max}$$

where Y is the observed RU, c is the concentration of the ligand, k_a is the association constant ($M\ s^{-1}$) and k_d is the dissociation constant (s^{-1}). B_{max} is the maximum signal from the ligand at saturation. The observed RU at time = 0 must be zero.

For the 1:2 state binding model, data were globally fitted to the following differential eqn using Tracedrawer (v 1.8) using numerical integration:

$$\frac{dAB}{dt} = (k_{a1} * c - k_{d1}) * AB \qquad \text{eqn 3}$$

$$\frac{dAC}{dt} = (k_{a2} * c - k_{d2}) * AC$$

$$Y = AB + AC$$

$$AB(0) = 0, AC(0) = 0, signal\ from\ saturated\ target = B_{max}\ and\ C_{max}$$

where Y is the observed RU, AB and AC are the individual observed RU of the two conformations of ligand immobilized on the chip, c is the concentration of the ligand, k_{a1} is the association constant of conformation state one($M\ s^{-1}$), k_{d1} is the dissociation constant of conformation state two(s^{-1}), k_{a2} is the association constant of conformation state two($M\ s^{-1}$), and k_{d2} is the dissociation constant of conformation state two(s^{-1}). B_{max} is the maximum signal from the ligand in conformation state one at saturation. C_{max} is the maximum signal from the ligand in conformation state two at saturation. The observed RU of the two conformations at time = 0 must be zero.

Goodness of fit was determined by a Chi-Square Test with the equation:

$$\chi^2 = \sum \frac{(o - e)^2}{e} \qquad \text{eqn 4}$$

where o is the observed value and e is the expected value.

TG2 - Ca^{2+} binding analysis with FURA-2

The K_d of Fura-2 for Ca^{2+} under our experimental conditions was determined fluorometrically using a ratiometric method (λ_1 = 340 nm, λ_2 = 380 nm). The K_d was determined using the equation:

$$[Ca^{2+}]_{free} = K_d \cdot \left\{\frac{R - R_{min}}{R_{max} - R}\right\} \cdot Q \qquad \text{eqn 5}$$

where R_{min} and R_{max} are the ratios of the fluorescence intensities at 340 and 380 nm determined at 0 μM and 39.5 μM Ca^{2+}, respectively. R is the ratio of florescence intensities measured at a specific Ca^{2+} concentration. K_d is the dissociation constant of Ca^{2+} binding for Fura-2. Finally, Q is a fluorescence correction factor, F_{380max}/F_{380min}, where F_{380max} and F_{380min} are the fluorescence intensities at 380 nm determined at 0 and 39.5 μM Ca^{2+}, respectively. The apparent K_d for Fura-2 was determined by extrapolation of the slope from log-log plots of fluorescent intensities at known standard concentrations of Ca^{2+} vs. log[Ca^{2+}]. Standard Ca^{2+} concentrations were prepared with an EGTA buffer system that follows the equation:

$$[Ca^{2+}]_{free} = K_d^{EGTA} \cdot \frac{[CaEGTA]}{[K_2EGTA]} \qquad \text{eqn 6}$$

Where K_d^{EGTA} is the dissociation constant of Ca^{2+} binding for EGTA [21]. CaEGTA was made by mixing 50 mM $CaCl_2$ and 50 mM EGTA. Standards were prepared in triplicate. Reported errors are ± standard deviation from triplicate experiments.

Ca^{2+} binding curves were generated by plotting the ratio of bound to total Ca^{2+} concentration ($[Ca^{2+}]_{Total}$-$[Ca^{2+}]_{Free}$/$[Ca^{2+}]_{Total}$) vs. [TG2] in μM. Equilibrium binding curves were fitted to either a one-site specific binding equation or an allosteric binding equation:

$$\frac{B_{max} * [A]^h}{{K_d}^h + [A]^h} \quad \text{eqn 7}$$

where B_{max} is the maximum binding fraction, [A] is the concentration of TG2, K_d is the binding constant, and h is the hill slope. One-site specific binding assumes the hill slope is equal to one. The B_{max} were not constrained to be below one.

Analysis of Dissociation Rates

Dissociation curves were fitted to the following decay equation:

$$Y = (Y_0 - Plateau) * 10^{(-K*x)} + Plateau \quad \text{eqn 8}$$

where Y is the signal response, Y_0 is the response at time = 0, plateau is the response at infinite times, K is the rate constant, and x is the observed time.

Results

Macromolecule Assembly in the Presence and Absence of Ca^{2+}

To investigate the interaction between TG2 and α-synuclein in various Ca^{2+} environments, we used Surface Plasmon Resonance (SPR). We first observed complex formation and dissociation in the absence of Ca^{2+} (10 mM EGTA) with varying α-synuclein. A sensorgram depicting the association and dissociation of the complex with TG2 on the chip surface was generated. We also tested the same interaction with varying TG2. Both TG2 and α-synuclein were dialyzed in an EGTA buffer to remove any endogenous Ca^{2+}. Sensorgrams with both interactions at 0 μM Ca^{2+} are shown in Figure 8A-B. Table 1 and 2 lists the resulting binding constants. A 1:2 state binding model was used when TG2 was on the chip and Langmuir's 1:1 state binding model for when α-synuclein was on the chip. The 1:2 state binding model assumes two conformational states of TG2 in solution form two separate complexes. Sensorgrams depicting complex formation with varying Ca^{2+} concentrations were also generated (Figure 9 and Figure 10). Some curves were removed from the fit due to calculated oversaturation on the chip (eqn 1). As a result, some plots only consist of three concentrations while others contain four. Graphs were fitted to the 1:2 state model and resulting binding constants were plotted (Figure 11).

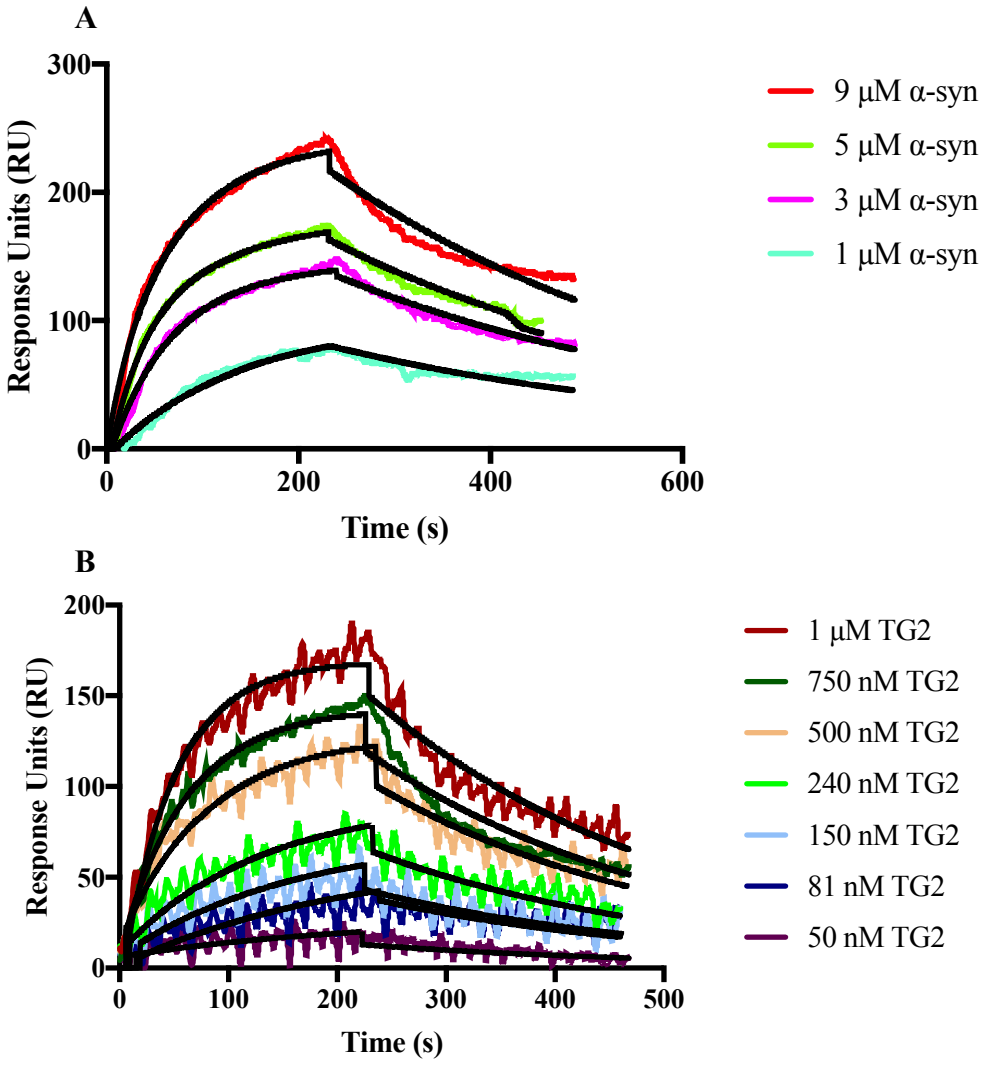

Figure 8A-B: **Binding of TG2 and α-synuclein in the presence of 10 mM EGTA.** (A) SPR sensorgram of complex with varying α-synuclein. Experiment conditions included a running buffer with 20 mM MOPS pH 7.2, 150 mM NaCl, 1 mM DTT, 10 mM EGTA. Data was globally fitted to a 1:2 state binding model (eqn 3). (B) SPR sensorgram of complex with varying TG2 under same experimental conditions. Data was fitted using Langmuir's 1:1 binding model (eqn 2).

Table 1: Binding constants from TG2: α-synuclein complex formation at 0 μM Ca^{2+} with varying α-synuclein

k_{a1} ($M\ s^{-1}$)	k_{d1} (s^{-1})	K_{D1} (M)	k_{a2} ($M\ s^{-1}$)	k_{d2} (s^{-1})	K_{D2} (M)	Chi-Square
5390 ± 224	$2.20 * 10^{-3} \pm 3.90 * 10^{-6}$	$4.08 * 10^{-7} \pm 1.77 * 10^{-8}$	1240± 347	$2.50 * 10^{-3} \pm 6.38 * 10^{-7}$	$2.01 * 10^{-6} \pm 6.08 * 10^{-7}$	32.77

Table 2: Binding constants from TG2: α-synuclein complex formation at 0 μM Ca^{2+} with varying TG2

k_a ($M\ s^{-1}$)	k_d (s^{-1})	K_D (M)	Chi-Square
18900 ± 125	$3.46*10^{-3} \pm 2.16*10^{-6}$	$1.84*10^{-7} \pm 1.33*10^{-9}$	54.58

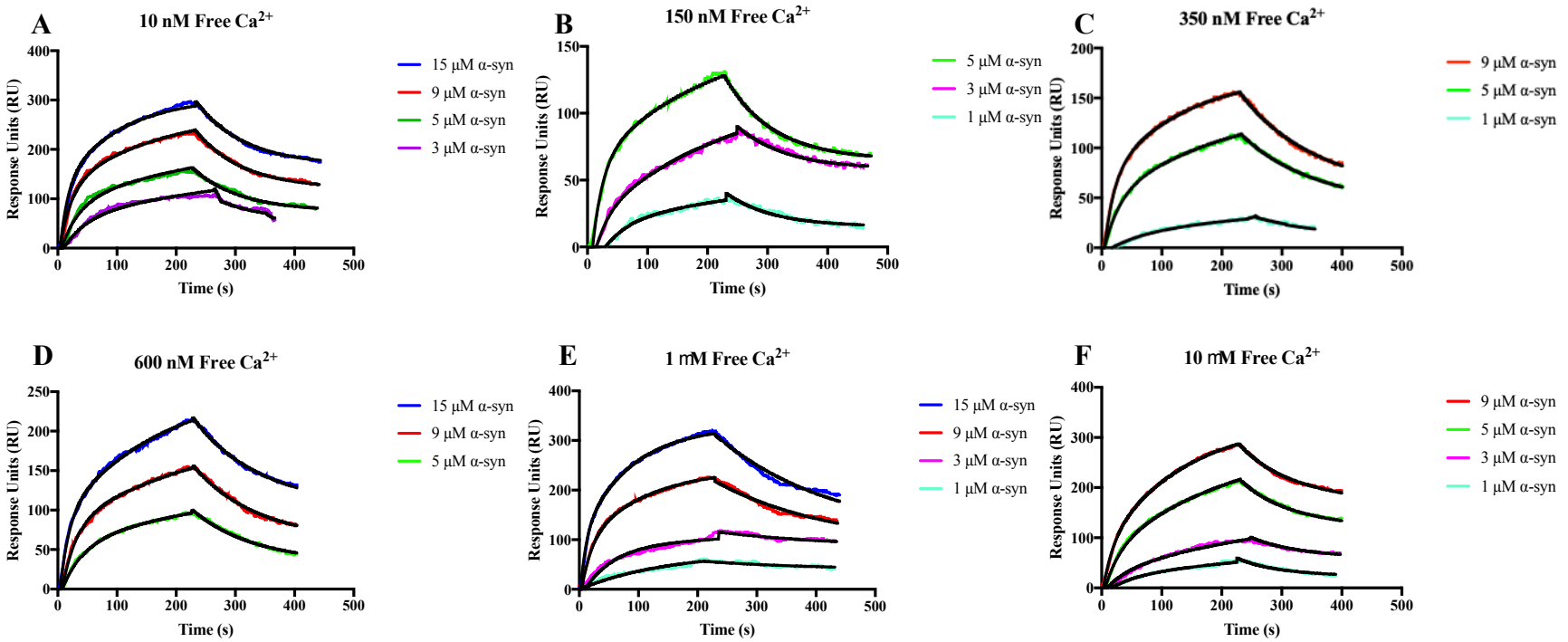

Figure 9A-F: **TG2: α-synuclein complex formation in low Ca^{2+} environments.** SPR sensorgrams of complex formation with varying α-synuclein ranging from 10 nM to 10 µM free Ca^{2+}. Experiment conditions consisted of a running buffer with 20 mM MOPS pH 7.2, 150 mM NaCl, 1 mM DTT, 10 mM EGTA. Data was fitted using a 1:2 state binding model (eqn 3).

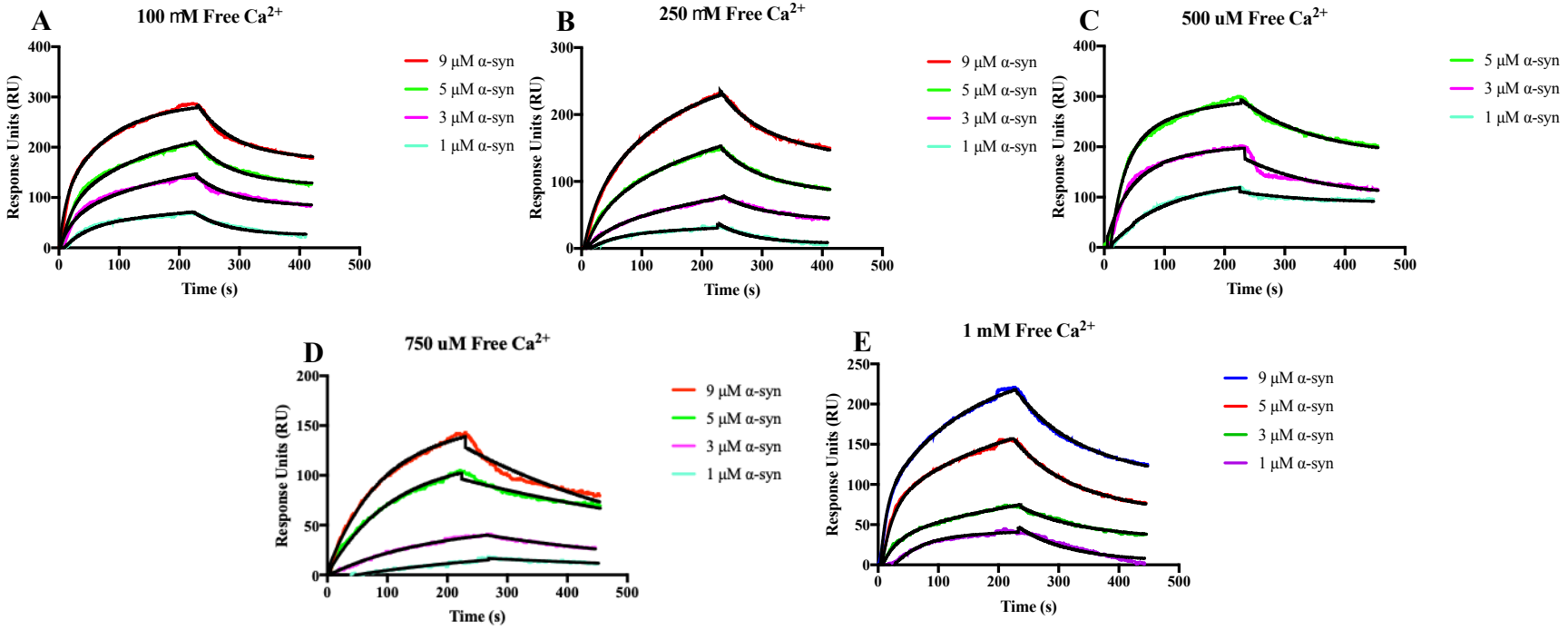

Figure 10A-E: **TG2: α-synuclein complex formation in high Ca^{2+} environments.** SPR sensorgrams of complex formation with varying α-synuclein ranging from 100 µM to 1 mM free Ca^{2+}. Experiment conditions consisted of a running buffer with 20 mM MOPS pH 7.2, 150 mM NaCl, 1 mM DTT, 10 mM EGTA. Data was fitted using a 1:2 state binding model (eqn 3).

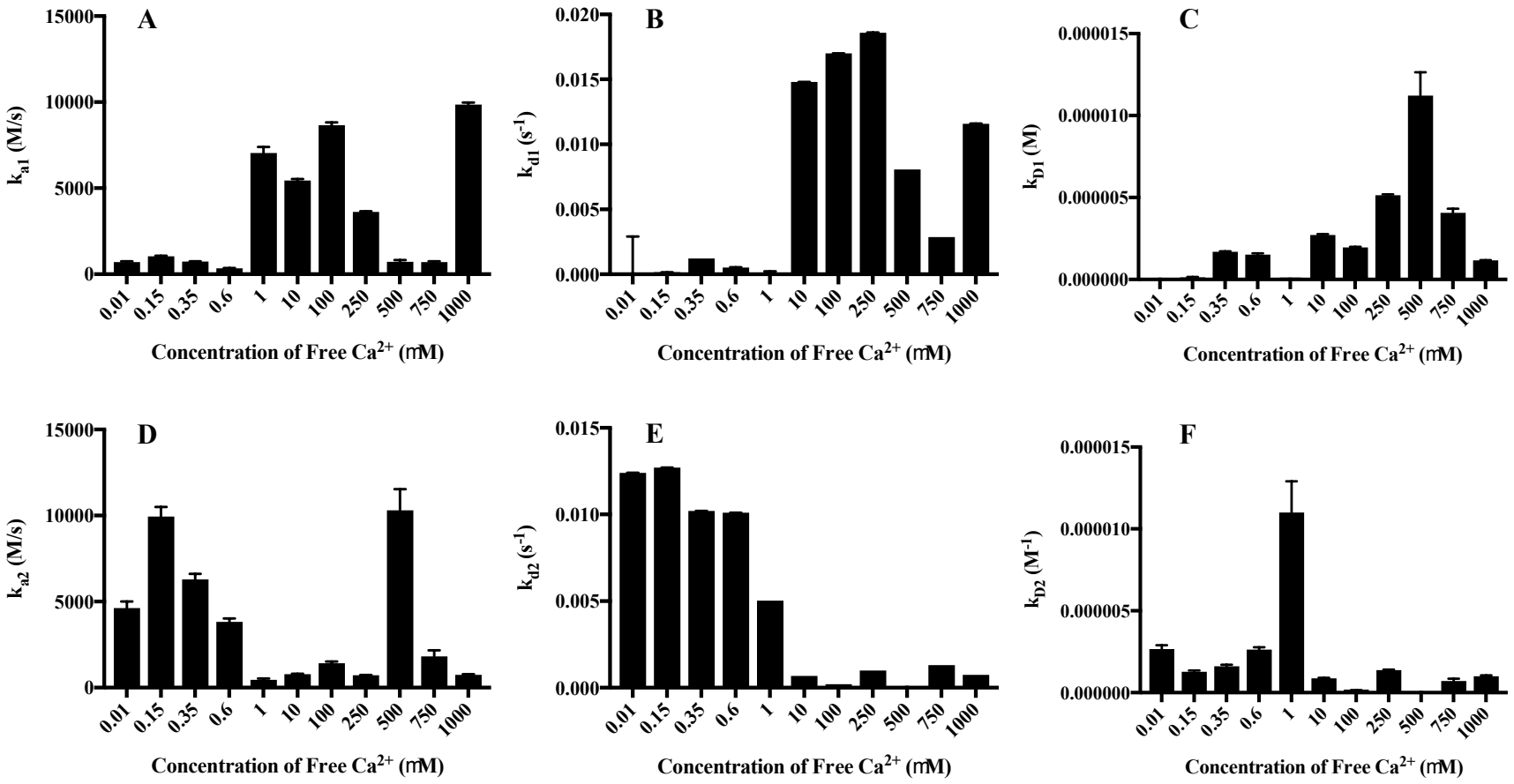

Figure 11A-F: **Resulting binding constants from complex formation in various Ca^{2+} environments.** Resulting binding constants derived from a 1:2 state binding model (eqn 3). The figures display the association, dissociation, and equilibrium constants of the two conformations of TG2.

Table 3: Binding constants from TG2: α-synuclein complex formation at various Ca^{2+} concentrations

	k_{a1} ($M\ s^{-1}$)	k_{d1} (s^{-1})	k_{D1} (M)	k_{a2} ($M\ s^{-1}$)	k_{d2} (s^{-1})	k_{D2} (M)	Chi-Square
10 nM Free Ca^{2+}	$7.03*10^{2} \pm 4.11*10^{1}$	$6.63*10^{-13} \pm 2.91*10^{3}$	$9.44*10^{-16} \pm 4.16*10^{0}$	$4.62*10^{3} \pm 3.90*10^{2}$	$1.24*10^{-2} \pm 2.46*10^{-7}$	$2.67*10^{-6} \pm 2.27*10^{-7}$	18.96
150 nM Free Ca^{2+}	$1.04*10^{3} \pm 2.53*10^{1}$	$4.86*10^{-5} \pm 1.13*10^{-4}$	$4.66*10^{-8} \pm 1.09*10^{-7}$	$9.94*10^{3} \pm 5.56*10^{2}$	$1.27*10^{-2} \pm 3.27*10^{-7}$	$1.28*10^{-6} \pm 7.20*10^{-8}$	3.89
350 nM Free Ca^{2+}	$7.29*10^{2} \pm 1.33*10^{1}$	$1.23*10^{-3} \pm 1.92*10^{-6}$	$1.69*10^{-6} \pm 3.36*10^{-8}$	$6.29*10^{3} \pm 3.13*10^{2}$	$1.02*10^{-2} \pm 1.60*10^{-7}$	$1.62*10^{-6} \pm 8.08*10^{-8}$	2.03
600 nM Free Ca^{2+}	$3.46*10^{2} \pm 1.17*10^{1}$	$5.26*10^{-4} \pm 7.69*10^{-6}$	$1.52*10^{-6} \pm 7.39*10^{-8}$	$3.82*10^{3} \pm 2.00*10^{2}$	$1.01*10^{-2} \pm 1.13*10^{-7}$	$2.63*10^{-6} \pm 1.38*10^{-7}$	4.01
1 μM Free Ca^{2+}	$7.04*10^{3} \pm 3.54*10^{2}$	$9.52*10^{-15} \pm 2.33*10^{4}$	$1.35*10^{-8} \pm 3.33*10^{0}$	$4.57*10^{2} \pm 7.68*10^{1}$	$5.03*10^{-3} \pm 1.34*10^{-7}$	$1.10*10^{-5} \pm 1.90*10^{-6}$	20.75
10 μM Free Ca^{2+}	$5.43*10^{3} \pm 8.84*10^{1}$	$1.48*10^{-2} \pm 4.70*10^{-7}$	$2.72*10^{-6} \pm 4.44*10^{-8}$	$7.80*10^{2} \pm 2.34*10^{1}$	$6.87*10^{-4} \pm 4.49*10^{-7}$	$8.81*10^{-7} \pm 2.71*10^{-8}$	6.09
100 μM Free Ca^{2+}	$8.66*10^{3} \pm 1.55*10^{2}$	$1.70*10^{-2} \pm 1.04*10^{-6}$	$1.96*10^{-6} \pm 3.53*10^{-8}$	$1.40*10^{3} \pm 1.03*10^{2}$	$1.82*10^{-4} \pm 4.13*10^{-6}$	$1.30*10^{-7} \pm 1.26*10^{-8}$	15.84
250 μM Free Ca^{2+}	$3.62*10^{3} \pm 3.89*10^{1}$	$1.86*10^{-2} \pm 2.83*10^{-7}$	$5.14*10^{-6} \pm 5.54*10^{-8}$	$7.23*10^{2} \pm 1.34*10^{1}$	$9.96*10^{-4} \pm 1.60*10^{-7}$	$1.38*10^{-6} \pm 2.57*10^{-8}$	2.57
500 μM Free Ca^{2+}	$7.22*10^{2} \pm 9.11*10^{1}$	$8.07*10^{-3} \pm 1.21*10^{-6}$	$1.12*10^{-5} \pm 1.43*10^{-6}$	$1.03*10^{4} \pm 1.23*10^{3}$	$1.63*10^{-13} \pm 1.12*10^{3}$	$1.58*10^{-17} \pm 1.10*10^{-1}$	31.64
750 μM Free Ca^{2+}	$7.05*10^{2} \pm 4.18*10^{1}$	$2.87*10^{-3} \pm 1.12*10^{-6}$	$4.07*10^{-6} \pm 2.44*10^{-7}$	$1.82*10^{3} \pm 3.43*10^{2}$	$1.31*10^{-3} \pm 1.36*10^{-6}$	$7.21*10^{-7} \pm 1.41*10^{-7}$	6.50
1 mM Free Ca^{2+}	$9.86*10^{3} \pm 1.08*10^{2}$	$1.16*10^{-2} \pm 5.38*10^{-7}$	$1.17*10^{-6} \pm 1.29*10^{-8}$	$7.44*10^{2} \pm 3.15*10^{1}$	$7.49*10^{-4} \pm 6.10*10^{-7}$	$1.01*10^{-6} \pm 4.35*10^{-8}$	4.30

TG2 Complex Formation with Casein and Cbz-Gln-Gly

To investigate the non-physiological and uncommon interactions with TG2, we used SPR to study complex formation with Cbz-Gln-Gly and casein in various Ca^{2+} environments. Cbz-Gln-Gly showed unfavorable binding with TG2 in both Ca^{2+} free and Ca^{2+} rich environments (Figure 12A-C). Data were not fitted to due to a poor response signal. TG2 interactions with casein however showed complex formation in both Ca^{2+}-free and Ca^{2+} rich environments (Figure 13A and 13B). Resulting binding constants from the 1:2 state fitting model are displayed in Table 4.

Effect of Ionic Strength on TG2: α-synuclein complex formation

Current studies have used a constant physiological based ionic strength to investigate complex formation (0.3 M ionic strength). To determine the effect on the association of the TG2: α-synuclein complex, we used SPR to establish this relationship. Sensorgrams showing complex formation at various ionic strengths were generated (Figure 14). Resulting binding constants are displayed in Table 5.

TG2 Binding Interactions with Ca^{2+} using FURA-2 as a Fluorescent Probe

TG2 interactions with Ca^{2+} were further investigated using FURA-2 to measure Ca^{2+} uptake at low concentrations. Ca^{2+} interactions between C277A, and the C277A: α-synuclein complexes were also studied (Figure 15A-F). Results were fitted to either the one-site specific hyperbolic equation or the allosteric binding equation (eqn 7; Table 6).

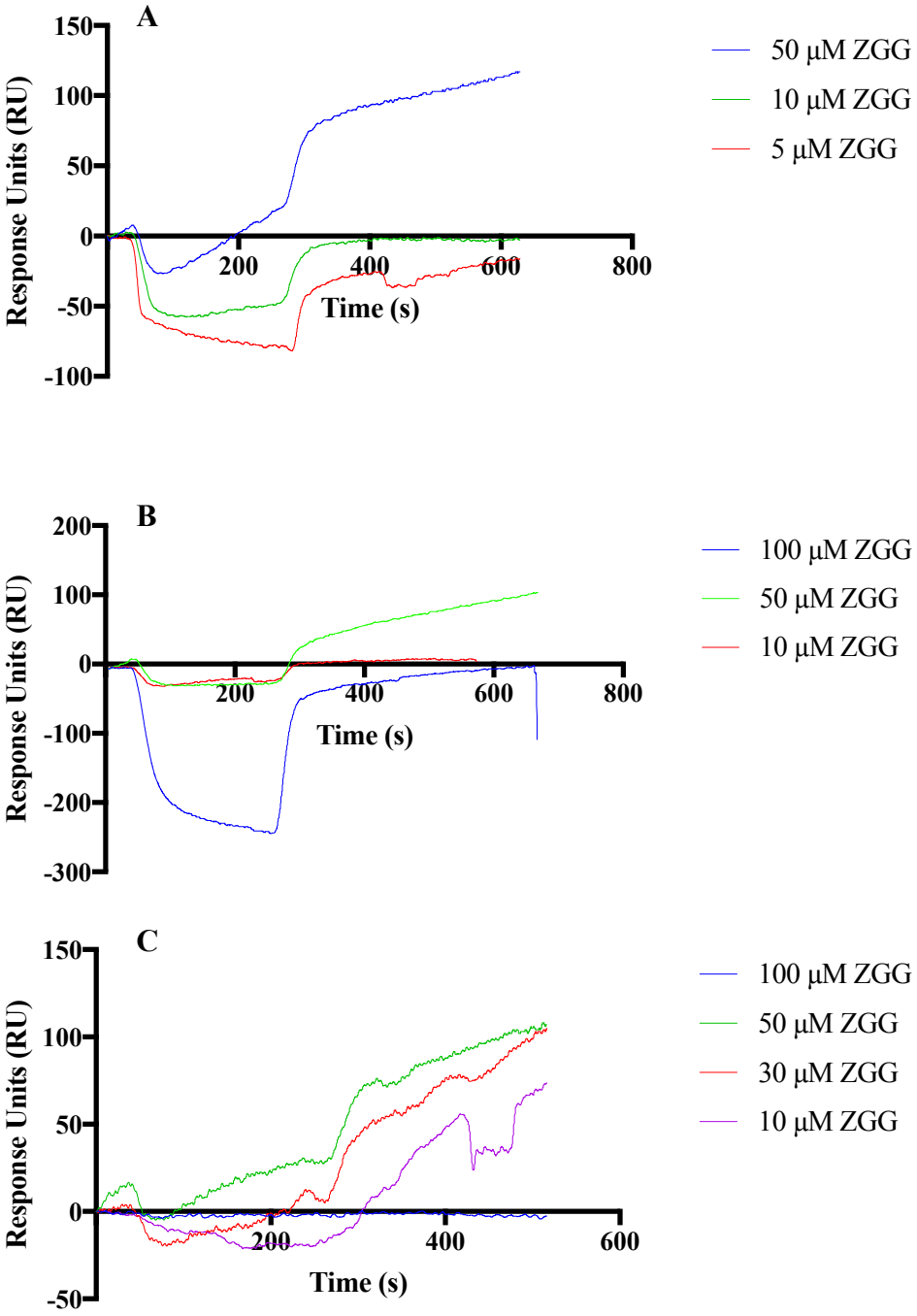

Figure 12A-C: **TG2 interactions with Cbz-Gln-Gly at various Ca^{2+} concentrations**. SPR Sensorgraphs of TG2 interacting with ZGG at 0 µM, 1 mM and 10 mM free Ca^{2+}, respectively. Typical experimental conditions consisted of a running buffer with 20 mM MOPS pH 7.2, 150 mM NaCl, and 1 mM DTT.

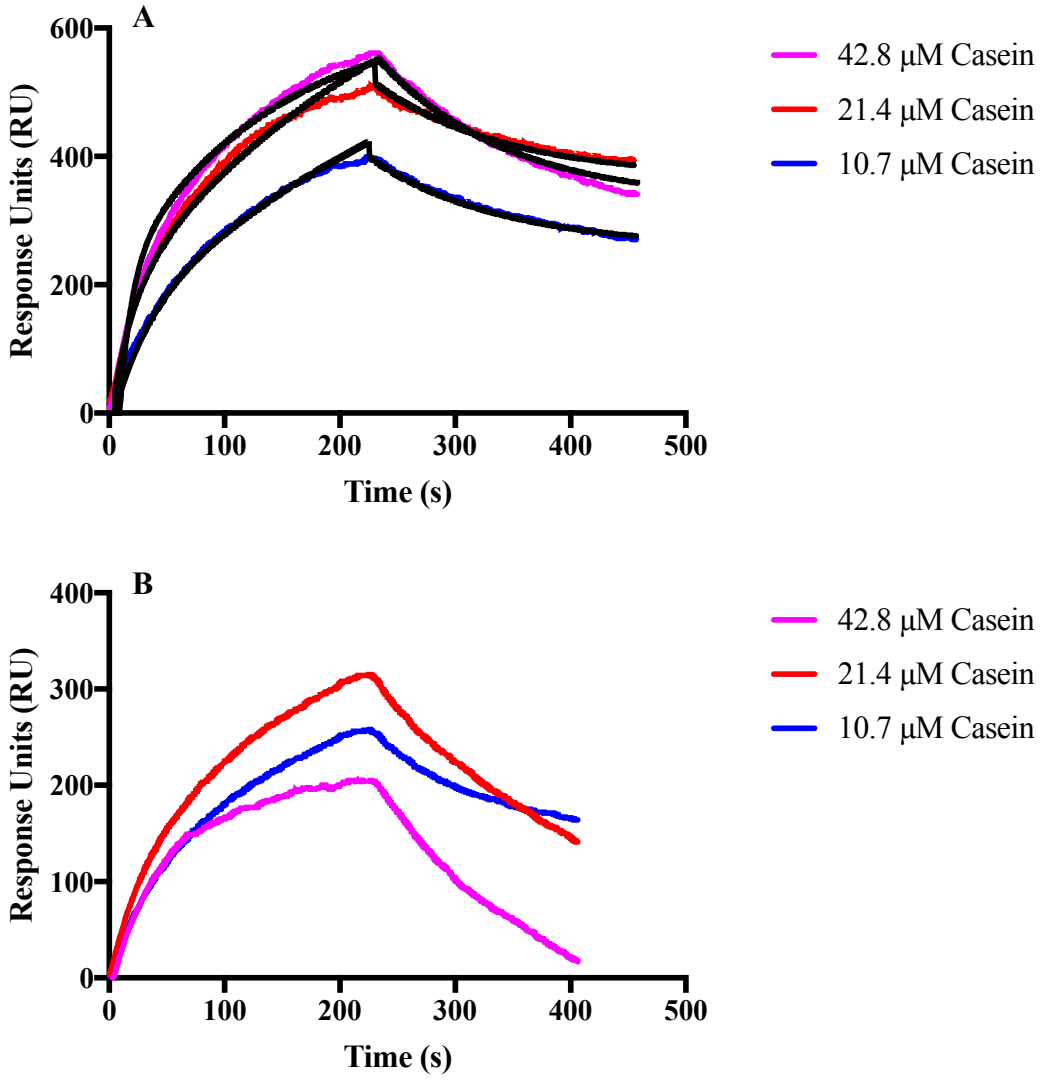

Figure 13A-B: **TG2 interactions with casein at various Ca^{2+} concentrations**. SPR sensorgrams of TG2 complex formation with casein at 0 µM and 1 mM free Ca^{2+}, respectively. Typical experimental conditions consisted of a running buffer with 20 mM MOPS pH 7.2, 150 mM NaCl, and 1 mM DTT. Data was fit to Langmuir's 1:2 binding model (eqn 3).

Table 4: Binding constants derived from TG2: casein complex formation at 0 μM Free Ca^{2+}.

	k_{a1} ($M\ s^{-1}$)	k_{d1} (s^{-1})	k_{D1} (M)	k_{a2} ($M\ s^{-1}$)	k_{d2} (s^{-1})	k_{D2} (M)	Chi-Square
Casein 0 μM Free Ca^{2+}	$2.06*10^{3} \pm 9.72*10^{2}$	$8.95*10^{-3} \pm 3.42*10^{-6}$	$4.34*10^{-6} \pm 2.63*10^{-6}$	$1.76*10^{2} \pm 8.41*10^{1}$	$5.38*10^{-10} \pm 2.41*10^{0}$	$1.01*10^{-12} \pm 4.35*10^{-2}$	148.75

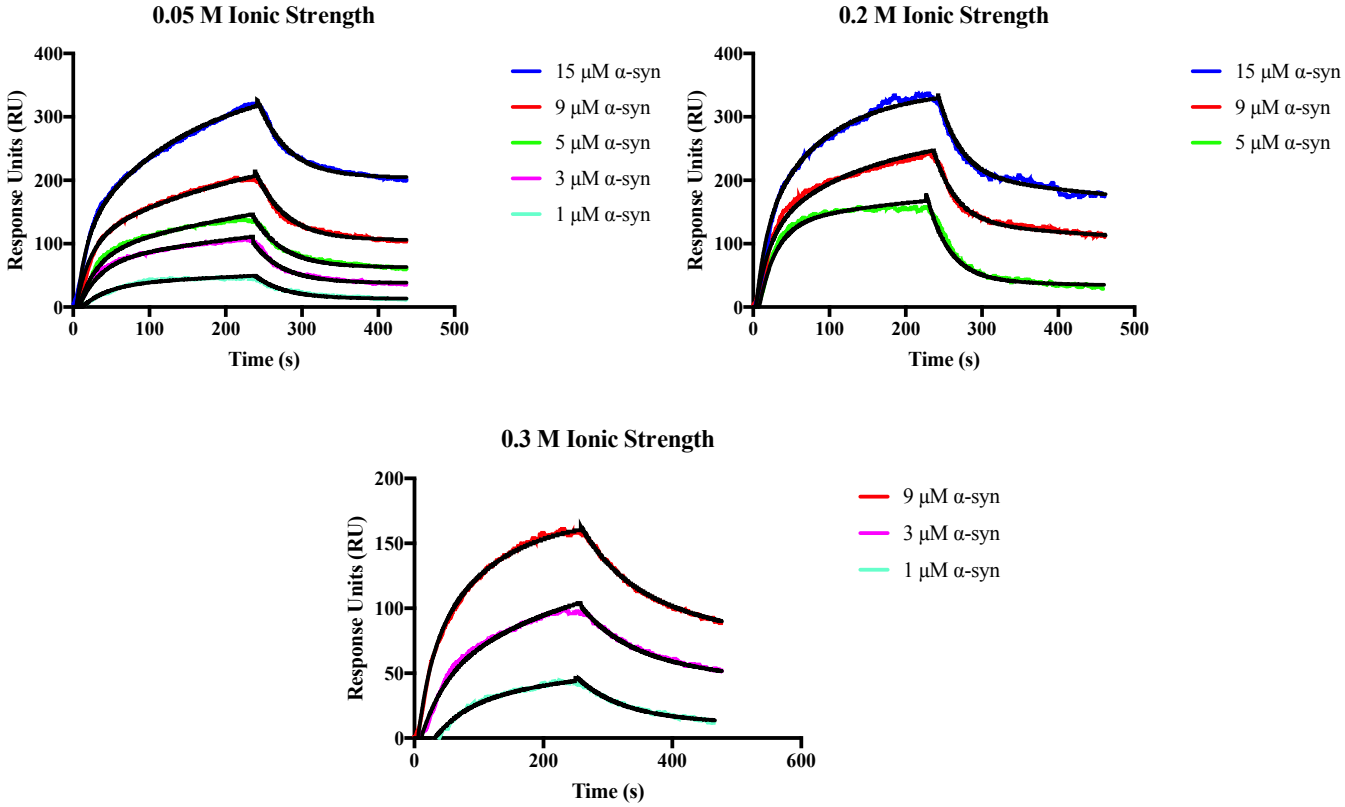

Figure 14A-B: **Effects of complex formation with varying ionic strengths**. SPR sensorgrams of TG2 complex formation with casein at 0 µM and 1 mM free Ca^{2+}, respectively. Typical experimental conditions consisted of a running buffer with 20 mM MOPS pH 7.2, 1 mM DTT, and 10 mM EGTA. Data was fitted to a 1:2 binding model (eqn 3).

Table 5: Binding constants derived from TG2: α-synuclein complex formation with varying ionic strength

	k_{a1} ($M\ s^{-1}$)	k_{d1} (s^{-1})	k_{D1} (M)	k_{a2} ($M\ s^{-1}$)	k_{d2} (s^{-1})	k_{D2} (M)	Chi-Square
0.05 M Ionic Strength	$3.23*10^{3} \pm 2.77*10^{1}$	$2.57*10^{-2} \pm 2.70*10^{-7}$	$7.97*10^{-6} \pm 6.84*10^{-8}$	$4.69*10^{2} \pm 3.81*10^{1}$	$3.20*10^{-13} \pm 9.90*10^{1}$	$6.82*10^{-16} \pm 2.12*10^{-1}$	9.87
0.2 M Ionic Strength	$7.17*10^{2} \pm 8.17*10^{1}$	$6.47*10^{-4} \pm 1.85*10^{-5}$	$9.01*10^{-7} \pm 1.30*10^{-7}$	$2.44*10^{3} \pm 1.73*10^{2}$	$3.33*10^{-2} \pm 1.73*10^{-7}$	$1.37*10^{-5} \pm 9.75*10^{-7}$	36.94
0.3 M Ionic Strength	$3.23*10^{3} \pm 2.38*10^{1}$	$8.85*10^{-4} \pm 3.23*10^{-6}$	$8.46*10^{-7} \pm 2.24*10^{-8}$	$4.40*10^{3} \pm 2.27*10^{2}$	$1.32*10^{-2} \pm 1.83*10^{-7}$	$3.05*10^{-6} \pm 1.58*10^{-7}$	3.57

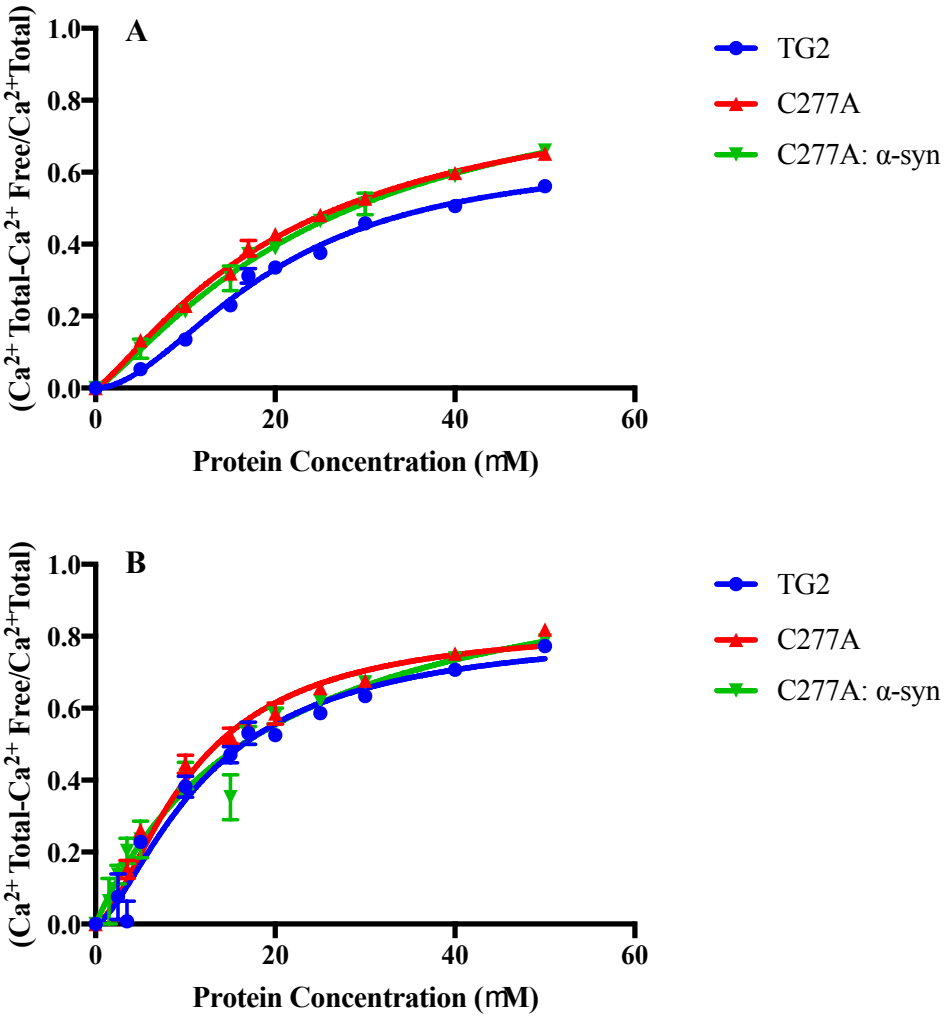

Figure 15A-E: **The effects of Ca^{2+} binding on TG2 and mutants**. Ca^{2+} binding to TG2 in 1 µM (A) and 5 µM (B) free Ca^{2+}, respectively. α-synuclein concentration was kept constant at 5 µM. Typical experimental conditions consisted of a 5x EGTA buffer system with 150 mM MOPS pH 7.2, 500 mM NaCl, and 50 mM EGTA. 2 µM of BSA was also added to each sample. Data was fitted to the allosteric equations (eqn 8), with the preferred model being shown. Data was recorded in triplicate. Error bars represent +/- standard deviation.

Table 6: Binding constants derived from TG2: Ca^{2+} binding using FURA-2 as fluorescent probe

	B_{max}	k_d (μM)	h	Goodness of Fit (R-Square)
WT TG2 at 1 μM Free Ca^{2+}	0.66± 0.03	20± 1	1.8± 0.1	0.9915
WT TG2 at 5μM Free Ca^{2+}	0.83± 0.05	24± 4	1.5± 0.2	0.9681
C277A at 1 μM Free Ca^{2+}	0.88± 0.05	22± 2	1.3± 0.08	0.9945
C277A at 5μM Free Ca^{2+}	0.83± 0.05	11± 1	1.6± 0.2	0.9575
C277A: α-synuclein complex at 1μM Free Ca^{2+}	0.95± 0.08	26± 4	1.2± 0.1	0.9921
C277A: α-synuclein complex at 5μM Free Ca^{2+}	1.1± 0.06	20± 2	One-site specific model preferred	0.9657

Discussion

We first investigated TG2 α-synuclein and complex formation in a Ca^{2+} free environment using Surface Plasmon Resonance (SPR). We wanted to confirm our proposed model of complex formation being capable without Ca^{2+}. We believe that previous studies generated a different model due to the use of both non-physiological and uncommon substrates.

We found that complex formation is obtainable in the absence of Ca^{2+}. This result directly challenges the currently accepted model of Ca^{2+} inducing conformational changes to TG2 alone. Because Ca^{2+} is required for catalytic activity, it is believed that Ca^{2+} must play a role elsewhere in the mechanism. The resulting Chi-Square of the two fits were found to be 32.77 with TG2 on the chip and 40.32 with α-synuclein. We think that these high deviations of the fits are due to a more complicated binding mechanism that our models do not account for. The 1:2 state binding model states there are two conformational states of TG2, each capable of binding α-synuclein with different k_a and k_d. Although we understand that TG2 exist as two forms in solution, we believe that the mechanism of complex formation is more complicated than this model allows [32,36]. We propose three possible models of TG2 complex formation that we believe to be a more accurate representation (Figure 17A-C). As a result of preliminary studies, each model assumes that the dissociation of the complex is a single exponential (Figure 16). Model B is favored, as one dissociation from one conformational state is most likely. α-Synuclein's intrinsically disordered structure could also make additional conformational changes to the complex more likely. The conformational changes could be thermodynamically driven, in which complex dissociation would only be obtainable at a once a specific conformation state is obtained.

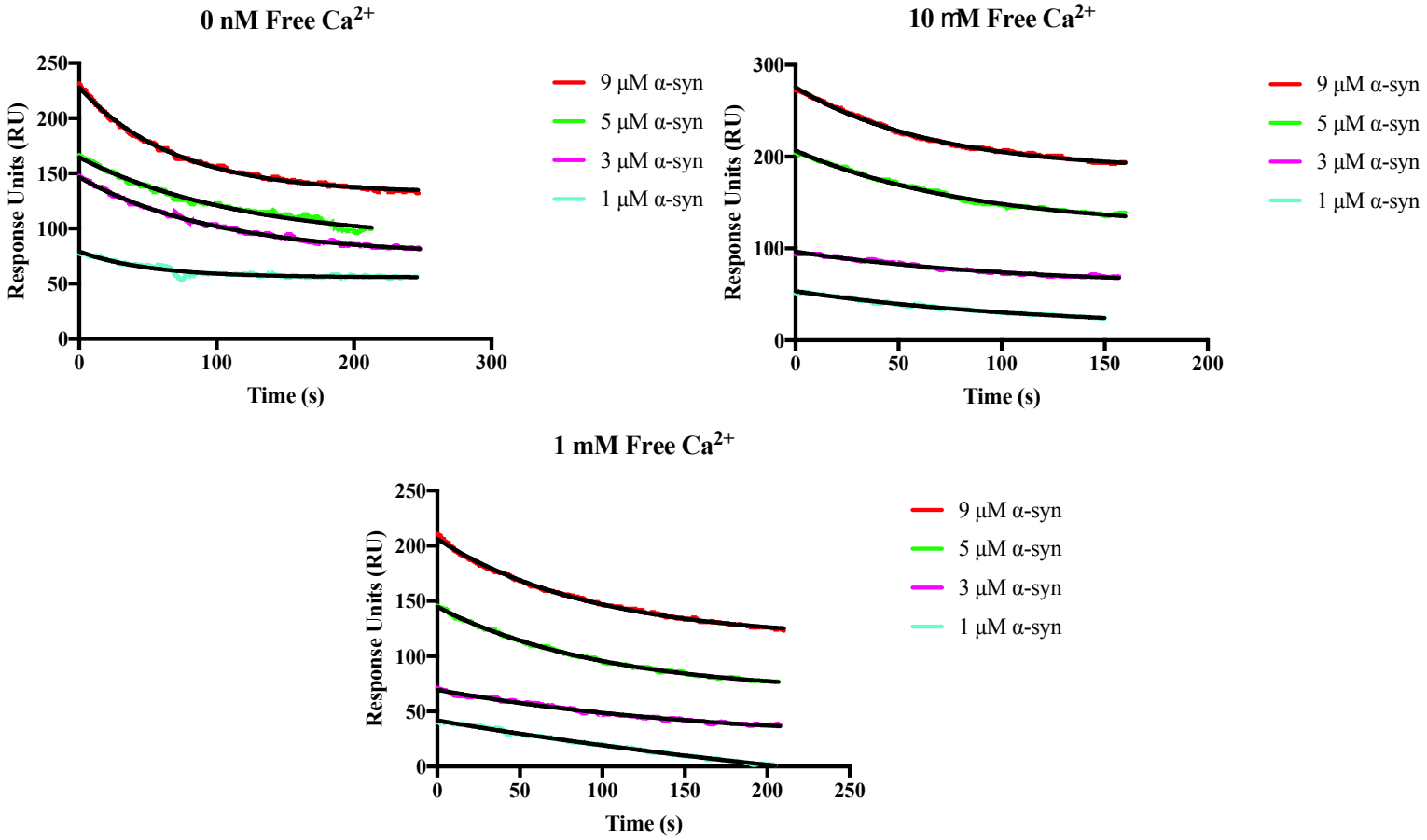

Figure 16: **Effects of α-synuclein concentration on dissociation rates of TG2: α-synuclein complex.** Plotted K_{obs} from dissociation against α-synuclein concentration. K_{obs} were determined from eqn (9).

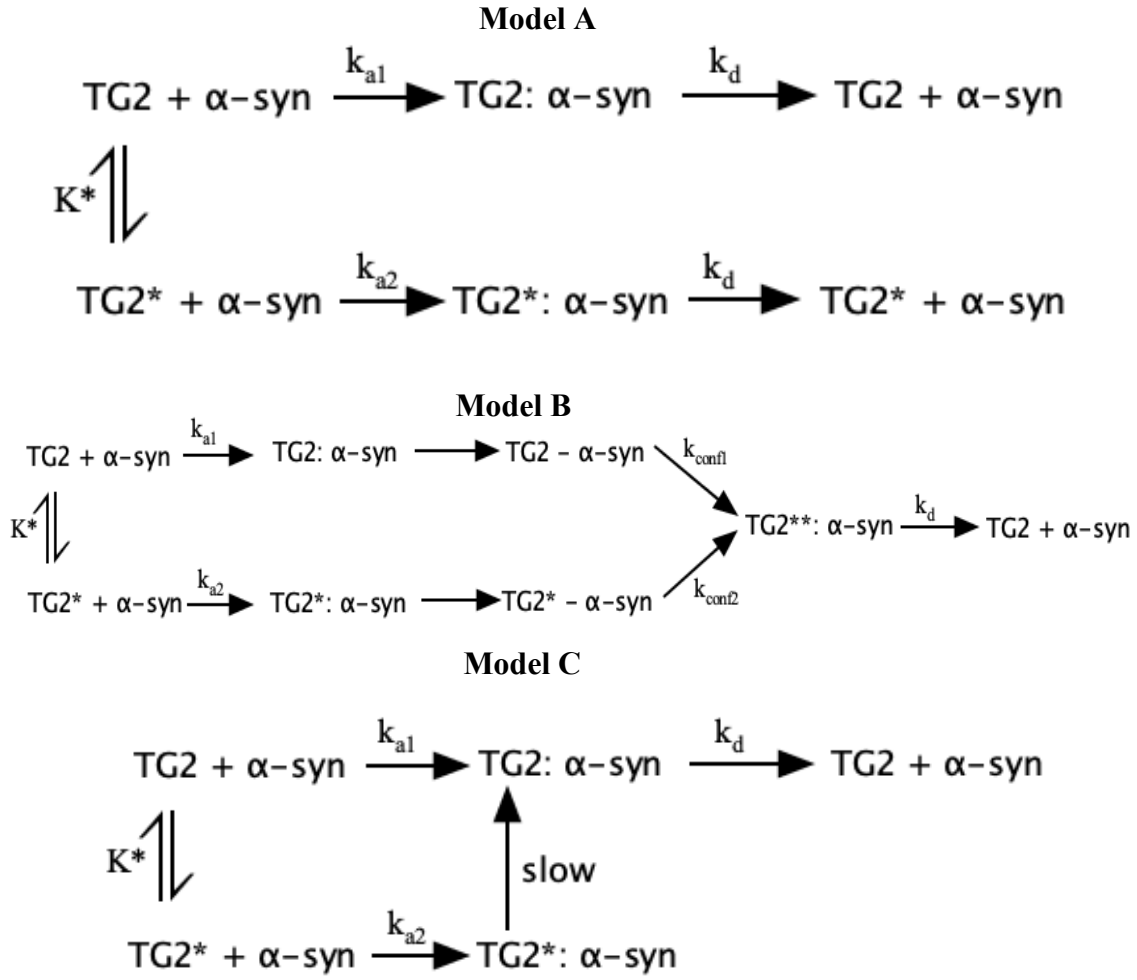

Figure 17A-C: **Potential mechanistic models for TG2: α-synuclein complex formation**. We believe that TG2 complex formation is more intricate than what the 1:2 state binding model offers. In these models, k_a represents the association constant, k_d represents the dissociation constant, k_{conf} represents the constant regarding conformational change to the enzyme: substrate complex, and K* represents the equilibrium constant of the two states of the enzyme. (A) The two conformation states TG2 exist in are allowed to form and dissociate the complex. This model assumes $k_{d1} = k_{d2}$. (B) The two states of TG2 can form complexes however a secondary conformational change occurs in order for dissociation to proceed. (C) Both states of TG2 can form the complex however only one conformation can dissociate. All three models assume the two states are in equilibrium in buffer.

Since we believe Model B is representative of what is actually occurring, it is important to note that the second conformational change could potentially be a rate determining step. For the sake of simplicity, the model does not show interchanging between the two complexes. It is believed that α-synuclein is constantly in motion while being bound to TG2, and this extra flexibility could induce the constant restructuring of the complex. Each model also assumes that only one α-synuclein is binding to TG2. In physiological conditions, it is quite possible that actually two α-synuclein bind to TG2 [13]. This adds an extra layer of possible conformational changes and unique complexes that TG2 can have. In the future, SPR could be used to determine how many substrates are binding, as we could calculate our expected change in response based off of molecular weight.

When viewing the effects of Ca^{2+} on the formation of the complex it appears the varying Ca^{2+} concentrations are affecting the association rate constants. The association constants of the first conformational state of TG2 appears to favor higher concentrations of Ca^{2+}. The second state inversely appears to have an increase of the association rate constants in low concentrations of Ca^{2+}. Because our fitting model is not an accurate representation of the mechanism, we cannot make definite claims about the data. We are limited to observing trends in the rate constants. It would be insightful to compare the trends if the data gets fit to an appropriate model.

We also have to take a qualitative approach when analyzing the effect of ionic strength on the interactions between TG2 and α-synuclein. Looking at the characteristics of the curves, it does appear that decreasing ionic strength does allow complex formation to come to an equilibrium much quicker than at physiological conditions. As with the Ca^{2+} association data, it would be interesting to compare binding constants with a more accurate binding model.

Furthermore, we investigated TG2 interactions between Cbz-Gln-Gly and casein in both Ca^{2+} free and Ca^{2+} rich environments. Binding with Cbz-Gln-Gly showed little to no binding to TG2 in the absence of Ca^{2+}. As the Ca^{2+} levels increased, it appeared that binding became more favorable. This interaction is noteworthy as it appears to not follow the same binding mechanism as α-synuclein. The inability to form the complex in a Ca^{2+} free environment is uncharacteristic of a physiologically relevant substrate of TG2. It is also important to note that Cbz-Gln-Gly is much smaller than any physiological substrate (0.3 kDa) and its structure is simplistic, which could also be why its binding mechanism is unique. The small structure would likely not cause a conformational change to the complex upon binding. Due to the popular use of Cbz-Gln-Gly in determining transamidation activity, it is understood why the currently accepted model for TG2 activation states that it needs Ca^{2+} before the substrate can bind.

TG2's interactions with casein showed it can bind in both the absence and presence of Ca^{2+}. Casein was able to bind to TG2 in a Ca^{2+} free environment at a rate comparable to α-synuclein. Dissociation of the complex conversely appeared to be occurring at a faster rate. The versatility of TG2 allows for binding of a plethora of different proteins and molecules; however, it is expected that the stability of the different complexes formed will not be uniform. To add to this, the intrinsically disordered nature of α-synuclein allows for extra flexibility in finding a stable conformation of the TG2: α-synuclein complex [23]. Casein's structure does not follow this characteristic however, it is suspected that casein contains regions of disorder in areas that TG2 binding is likely.

FURA-2 studies investigate TG2- α-synuclein complex formation at different concentrations of Ca^{2+} and α-synuclein. We wanted to establish how TG2 interacts with α-synuclein and Ca^{2+}, specifically at low Ca^{2+} concentrations. We did not observe any significant

changes in Ca^{2+} binding between WT TG2 and C277A. Also, the binding constants obtained are not reflective of what we observe in the data. We believe that there is a large amount of error present in the fitting model. Because of this, we decided to take a qualitative approach in analyzing this data. What we can determine is that there is clear binding of Ca^{2+} to the apoenzyme. Although we do observe Ca^{2+} binding with TG2 alone, we don't believe it is overly-significant. We believe that binding is not catalytically competent.

Overall, in our studies we cannot make definite claims about our SPR data due to an inaccurate fitting model. We can however establish that (1) formation of the TG2: α-synuclein complex is obtainable in the absence of Ca^{2+}, (2) Ca^{2+} role in the activation of TG2 appears to differentially affect the association of the complex, and (3) ionic strength appears to affect the association of the complex. With increased Ca^{2+} levels being a characteristic of physiological damage in neuronal cells, it does appear that high concentrations of Ca^{2+} are affecting complex formation.

Section. 3 IDENTIFYING Ca^{2+} BINDING SITES AND CONFORMATIONAL CHANGES TO THE ENZYME: SUBSTRATE COMPLEX

Introduction

TG2 is capable of binding six Ca^{2+} ions. It is theorized that all six sites need to be occupied in order for catalytic turnover to take place [21]. The location of these Ca^{2+} binding sites however are in question. There are no known crystal structures of TG2 that have Ca^{2+} bound to the enzyme [21,27]. In addition, there is also uncertainty concerning if Ca^{2+} binding follows a cooperative mechanism. Ca^{2+} binding in certain regions of TG2 can potentially be more favorable depending on the conformational state of the enzyme. It is proposed that TG2 has a Ca^{2+} binding region that is buried near the catalytic core. Availability to this site is limited unless there is a conformational change that reveals the site [21,27]. This Ca^{2+} binding site is also hypothesized to be more critical for TG2 catalytic activity. Recent literature has predicted Ca^{2+} binding regions by performing multiple sequence alignments with transglutaminase 3 (TG3) and Factor XIII. These proteins are homologous to TG2 and contain Ca^{2+} binding regions that are evolutionary conserved. TG3 has three Ca^{2+} binding sites in its structure while Factor XIII contains one (Figure 18) [1,13]. Using the predicted Ca^{2+} binding regions, the literature created Ca^{2+} binding knock-outs of TG2. Along with the alignments, the study also looked the primary sequence of TG2 and proposed two more Ca^{2+} binding spots based off negatively charged regions [21]. The study synthesized Ca^{2+} knockout mutations of these sites as well (Figure 19; Table 7). The overall goal from the literature was to identify Ca^{2+} binding sites on TG2, in which they accomplished.

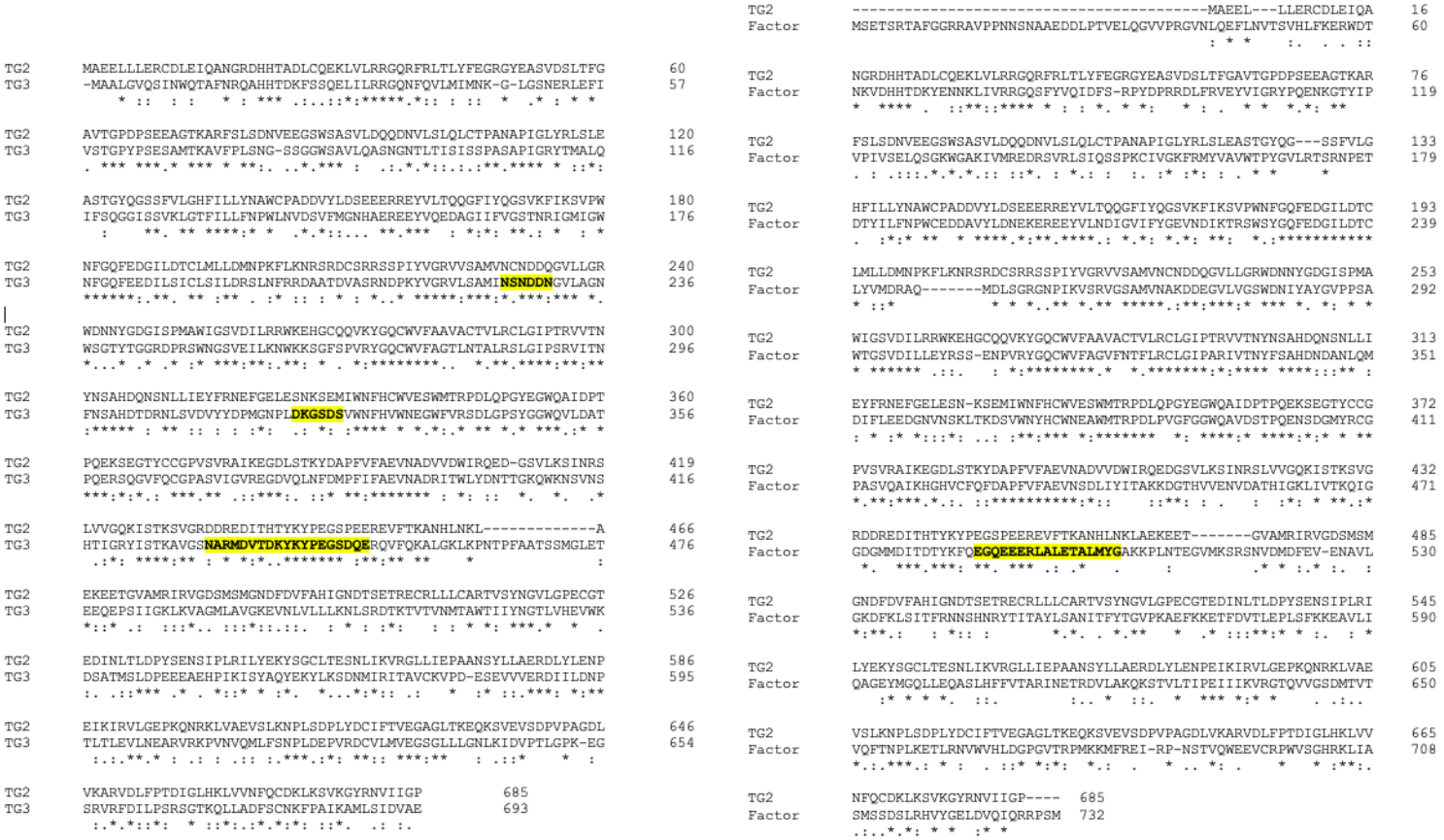

Figure 18: **Sequence alignments between TG2 homologs.** Global sequence alignments between TG2: TG3 and TG2: Factor XIII. Alignments were performed using Clustal. Ca^{2+} binding sites are marked in yellow.

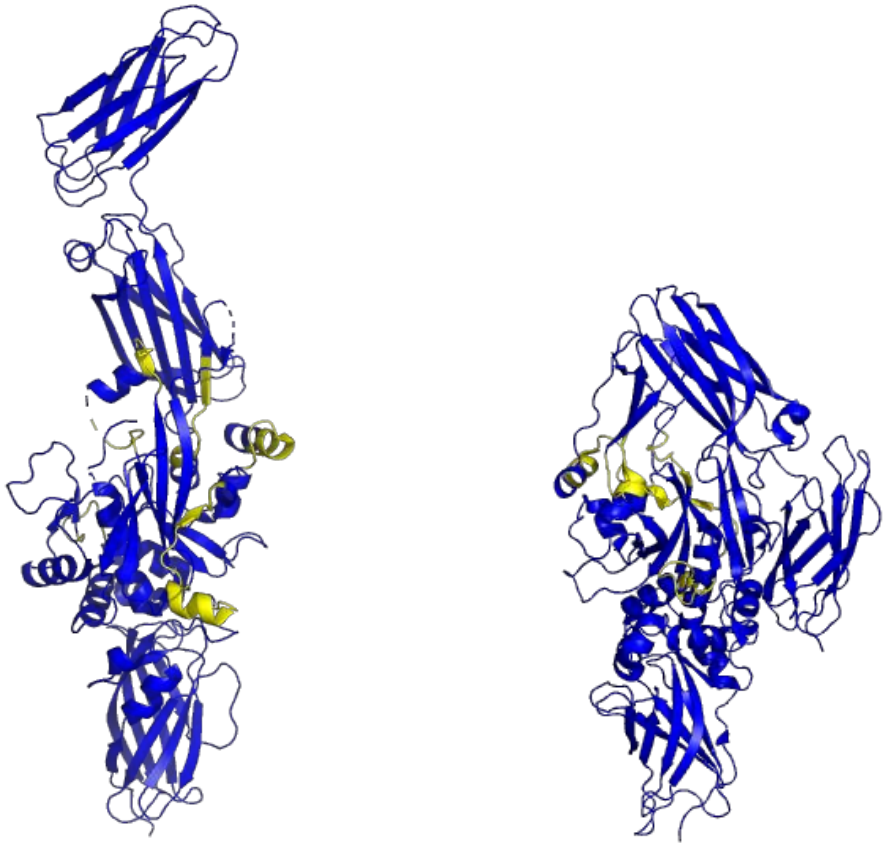

Figure 19: **Proposed Ca^{2+} binding sites.** Proposed Ca^{2+} binding sites in the "open" and "closed" conformations [17,27]. PDB 2Q3Z; 4PYG

Table 7: Mutagenized regions of TG2

Mutant	Original Sequence	Mutant Sequence
S1	228 V N C N D D Q G V	228 V S C S N N Q G V
S2A	395 A E V N A D V	395 A Q V S A N V
S2B	445 Y P E G S S E E R E A	445 Y P Q G S S Q Q R Q A
S3A	305 H D Q N S N L	305 H N Q S S S L
S3B	326 D K S E M I W N	326 D K S Q M I W N
S4	149 Y L D S E E E R Q E Y	149 Y L N S Q Q Q R Q Q Y
S5	432 G R D E R E D I T	432 G R N Q R Q N I T

An attempt to create our own mutations using bioinformatics was carried out. We aligned TG2 with calcium binding proteins that contain canonical binding regions (Table 8) [23]. Although the Ca^{2+} binding regions on TG2 are known to be noncanonical, it is possible that the regions could be semi-comparable to known Ca^{2+} binding regions on known proteins. Primarily, our objective was to confirm potential binding sites for TG2.

Table 8: List of calcium binding proteins used for alignments

Calcium Binding Protein	**Number of Calcium Binding Regions**	**Accession Number**
Calmodulin	4	P0DP23
Parvalbumin	2	P20472
Calcineurin	4	P63098
Calbindin	4	P05937
Recoverin	2	P35243
Neurocalcin	3	P61601
Calretinin	6	Q08331

There are also questions regarding TG2 structure after complex formation with Ca^{2+}. Preliminary data shows that TG2 undergoes a large conformational change during Ca^{2+} and substrate binding [20, 34]. However, the structure of the enzyme after complex formation has not been identified. We seek to find what happens structurally to TG2 after the full complex has formed, and also any further conformations when Ca^{2+} binds. We first wanted to observe

lanthanide interactions with TG2 and establish binding. Lanthanides are known to have the ability to bind to Ca^{2+} binding regions but with a higher affinity than Ca^{2+} [3-4,5,37]. They also have the ability to luminesce when excited, which can be measured by using a fluorometer. We have chosen Terbium as our model lanthanide for experimentation due to its easily observable emission wavelength at 546 nm.

Methods and Materials

Materials

All chemicals were purchased from VWR International (Radnor, PA).

Overexpression and Purification of protein

Refer to Section 2

Bioinformatics

Local sequence alignments were performed through the EMBOSS Water program [European Bioinformatics Institute]. Sequences of Transglutaminase 2 and other calcium binding proteins were blasted using UniProt and pasted into the Water program (BLOSUM62). The program provided the best fit and gave a description on the identity, similarity, and any gaps present in the alignment.

Terbium Binding Experiments

All binding experiments were performed on a spectrofluorometer. Experimental conditions consisted of 20 mM MOPS pH 7.2, 150 mM NaCl, 10 mM EGTA, and 1 mM DTT. Terbium stock concentration was 30 mM. TG2 concentration was kept at a constant 1.8 μM. C277A and α-synuclein concentrations were kept constant at 1 μM. Terbium was titrated at a constant volume of 1 μL. Terbium was excited at 259 nm and emission was measured from 250 to 700 nm. A reading was taken after each titration. Background emission was removed.

Results

Multiple sequence alignments between TG2 and known Ca^{2+} binding proteins

We investigated similarities between TG2 and Ca^{2+} binding proteins to identify possible sites for Ca^{2+} binding. The Ca^{2+} binding proteins used are known to contain canonical binding regions. Sequences were aligned in the water program and tested for similarities. Local sequence alignments are displayed in Table 9. Results of alignments are presented in Figure 20.

Measuring terbium binding by increase in luminescence

We investigated if additional conformational changes occur to the complex once Ca^{2+} is added. We used terbium to measure changes in luminescence. Resulting graphs from terbium emission at 524, 565, and 595 nm into TG2, α-synuclein, C277A, and the C277A: α-synuclein complex are shown below (Figure 21). Plots comparing maximum fluorescence to terbium concentration are also shown below (Figure 22). Plots were corrected for background signal.

Table 9: Local sequence alignments with TG2 and Ca^{2+} binding proteins

Calcium Binding Protein	Number of Calcium Binding Regions	Best Alignment (EMBOSS Water)	Identity	Similarity	Gaps	Score
Calmodulin	4	60 EGRGYEASVD 69 :|.||.:::.: 3 DGNGYISAAE 12	3/10 (30%)	7/10 (70%)	0/10 (0%)	22.0
Parvalbumin	2	177 QQGFI 181 :.||| 4 KSGFI 8	3/5 (60%)	4/5 (80%)	0/5 (0%)	17.0
Calcineurin	4	592 ERDLYLENPE 601 ::|.|:.|.| 3 DKDGYISNGE 12	4/10 (40%)	7/10 (70%)	0/10 (0%)	24.0
Calbindin	4	583 YLENPE 588 |||..| 7 YLEGKE 12	4/6 (66.7%)	4/6 (66.7%)	0/6 (0%)	20.0
Recoverin	2	187 DGILD 191 ||.|| 5 DGTLD 9	4/5 (80%)	4/5 (80%)	0/5 (0%)	21.0
Neurocalcin	3	116 RLSLE 120 :|||| 7 KLSLE 11	4/5 (80%)	5/5 (100%)	0/5 (0%)	19.0
Calretinin	6	114 LYRLSLE 120 |||..|| 6 LYRKDLE 12	5/7 (71.4%)	5/7 (71.4%)	0/7 (0%)	23.0

Figure 20: **Proposed Ca^{2+} binding sites from Ca^{2+} binding proteins.** Depiction of Ca^{2+} binding sites derived from the local sequence alignments with known Ca^{2+} binding protein. Ca^{2+} binding regions are proposed to be residues 60-69, 114-120, 177-190, and 583-601. Regions of interest are highlighted in magenta. Previously proposed Ca^{2+} binding sites are in yellow. PDB 2Q3Z

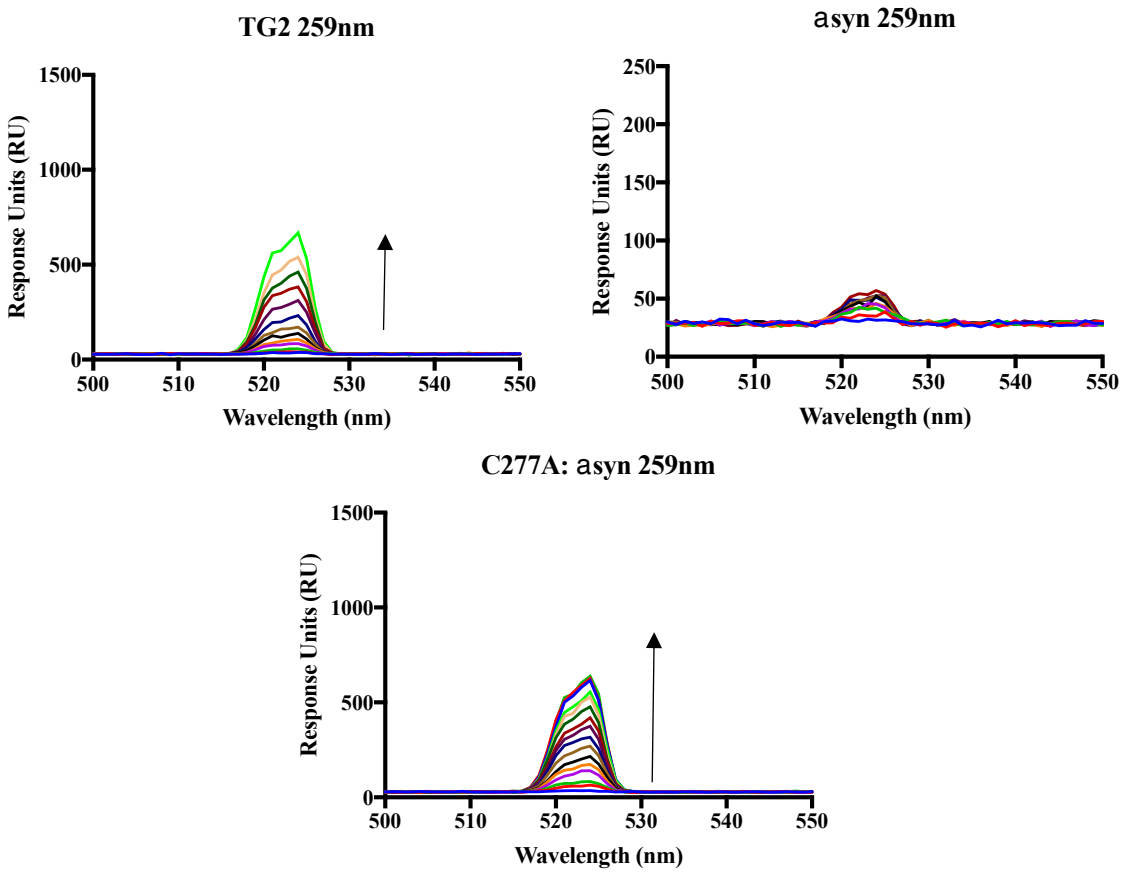

Figure 21: **Terbium binding with TG2.** Measured terbium emission at wavelength 524. Protein was excited at wavelengths 259, 280, and 295 nm. Arrows represent increased lanthanide binding to protein. Experimental conditions consisted of 20 mM MOPS pH 7.2, 150 mM NaCl, 10 mM EGTA, and 1 mM DTT. Terbium stock concentration was 30 mM. Starting TG2 concentration was 1.8 μM. Starting α-synuclein concentration was 1 μM. Starting C277A and α-synuclein concentration were 1.8 and 1 μM, respectively.

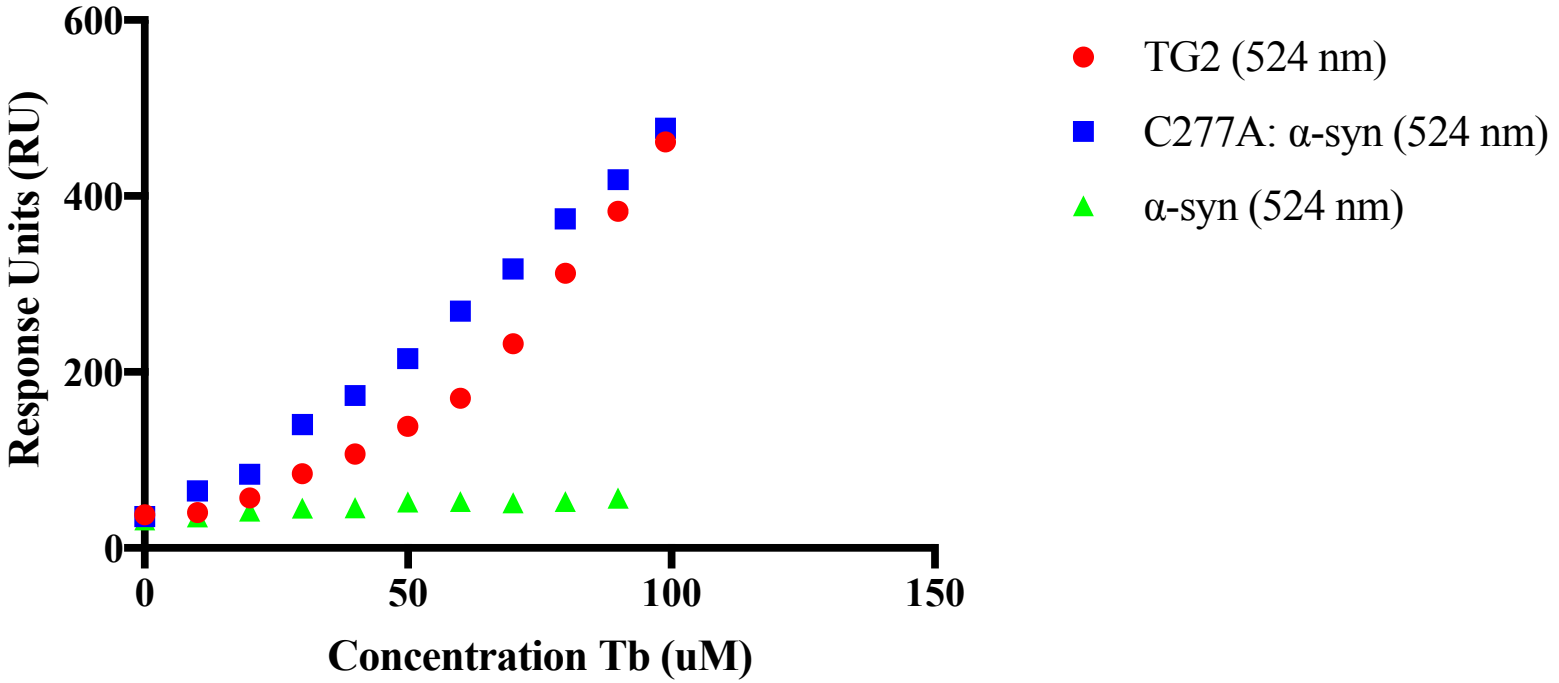

Figure 22: **Luminescence increases due to terbium binding.** Measured maximum luminescence from terbium binding with WT TG2, α-synuclein, and C277A: α-synuclein complex. Graphs focus on emission intensities at wavelength 524 nm.

Discussion

We attempted to identify Ca^{2+} binding sites on TG2 by comparing the protein sequence with other Ca^{2+} binding proteins that contained canonical regions. With the alignments of their respective Ca^{2+} binding regions, we were able to establish four regions of interest on TG2: amino acid residues 60-69, 114-120, 177-190, and 583-601. The regions contain a noteworthy amount of negatively charged residues, which would make sense for Ca^{2+} to have an affinity towards it. The region at 114-120 however only contained one negative residue (Glu 120). It is likely that this region has a weak interaction with Ca^{2+}. Regions also appear to be available on the surface of TG2's structure. It is noteworthy that none of the regions discovered overlapped with proposed Ca^{2-} binding sites from with previous literature. The regions are much more dispersed, as possible sites extend towards both of the termini. Although TG2 Ca^{2+} binding regions are considered non-canonical, it appears that TG2 shares similarities between canonical Ca^{2+} regions. It would be interesting to mutate the sites in these findings to determine if they have any adverse effect on complex formation or catalytic activity.

Terbium showed ample fluorescence in assumed binding between WT TG2 and the C277A: α-synuclein complex. Terbium mixed with α-synuclein did not result in a strong response. This could be due to the lack of aromatic residues in the structure of α-synuclein, which is required for luminescence emission. It is also possible that α-synuclein cannot bind terbium, as there is little evidence of α-synuclein containing Ca^{2+} binding regions. TG2 binding with terbium showed a noteworthy increase of luminescence at around 50 μM terbium concentration. The C277A: α-synuclein complex did not share this same characteristic, as it appears to stay linear throughout additional titrations. We further plan to perform Luminescence Resonance Energy Transfer (LRET) to observe the conformational change following Ca^{2+}

binding. LRET is similar to FRET, with the exception of emission being due to luminescence [8,18]. We also plan on synthesizing TG2 mutants with tryptophan residues near potential Ca^{2+} binding regions to optimize luminescence [14,18]. We don't know for sure if the increase is due to LRET or just a response to terbium binding. It would be insightful to use mutants that add tryptophan residues near proposed Ca^{2+} binding regions to determine if conformational changes are causing the inflation in the response.

In summary, (1) alignments of TG2 with canonical Ca^{2+} binding proteins produced four unique binding regions, and (2) terbium's interaction with TG2 and the TG2: α-synuclein showed noteworthy fluorescence. Identification of Ca^{2+} sites could be pivotal in our understanding in TG2's uncontrolled mechanism in Parkinson's disease.

Section 4. CONCLUSIONS AND FUTURE DIRECTIONS

In this study we investigated Ca^{2+} role in the mechanism of TG2 activation. We aimed to obtain a better understanding of its mechanism in order to understand how this enzyme works in neurodegenerative diseases. We first demonstrated that Ca^{2+} isn't necessary for TG2: α-synuclein complex formation. We went on to observe that varying Ca^{2+} and ionic strength appear to have an effect on the association of the complex. We will have to fit our data to a more accurate model before we can provide claims about the nature of the interactions. Our next step would be to investigate how Ca^{2+} is affecting the catalytic activity of the enzyme. It is hypothesized that Ca^{2+} could have a role in dictating transamidation activity of TG2. We would expect to see significant changes in transamidation rates if Ca^{2+} concentrations were altered. We also located possible Ca^{2+} binding sites on TG2 using bioinformatics. Mutations of these sites that knockout the ability for Ca^{2+} to bind can confirm lack of significance in the for specific sites in the binding mechanism. These mutations will also be beneficial in future kinetic experiments. Mutations can identify significant sites for kinetic activity as well as establish cooperation between binding sites [19]. Finally, we demonstrated the ability of terbium to interact with TG2 and the TG2: α-synuclein complex. We plan to synthesize mutations that add tryptophan residues near proposed Ca^{2+} binding regions to maximize LRET. This will give insight on further conformational changes to the enzyme: substrate complex after Ca^{2+} binding. We continue to learn about this enzyme in hopes of creating therapeutics designed to inhibit TG2 activity and prevent damage in neuronal cells.

REFERENCES

1) Ahvazi, B., Boeshans, K. M., Idler, W., Baxa, U., & Steinert, P. M. (2003). Roles of calcium ions in the activation and activity of the transglutaminase 3 enzyme. *Journal of Biological Chemistry, 278*(26), 23834-23841.
2) Bengoa-Vergniory, N., Roberts, R. F., Wade-Martins, R., & Alegre-Abarrategui, J. (2017). Alpha-synuclein oligomers: A new hope. *Acta Neuropathologica, 134*(6), 819-838. doi:10.1007/s00401-017-1
3) Bertini, I., Gelis, I., Katsaros, N., Luchinat, C., & Provenzani, A. (2003). Tuning the affinity for lanthanides of calcium binding proteins.*Biochemistry, 42*(26), 8011-8021.
4) Brittain, H. G., Richardson, F. S., & Martin, R. B. (1976). Terbium(III) emission as a probe of calcium(II) binding sites in proteins. *Journal of the American Chemical Society, 98*(25), 8255-8260.
5) Case, A., & Stein, R. L. (2003). Kinetic analysis of the action of tissue transglutaminase on peptide and protein substrates. *Biochemistry, 42*(31), 9466-9481. doi:10.1021/bi030084z
6) Causes & Statistics. (2018, October 17). Retrieved from https://parkinson.org/Understanding-Parkinsons/Causes-and-Statistics
7) Dell'Orco, D., & Koch, K. W. (2016). Fingerprints of Calcium-Binding Protein Conformational Dynamics Monitored by Surface Plasmon Resonance. *ACS chemical biology*, *11*(9), 2390-2397.
8) Dolino, D. M., Ramaswamy, S. S., & Jayaraman, V. (2014). Luminescence resonance energy transfer to study conformational changes in membrane proteins expressed in mammalian cells. *Journal of Visualized Experiments,* (91), 51895.

9) Dominy, B. N., Perl, D., Schmid, F. X., & Brooks, C. L. (2002). *The effects of ionic strength on protein stability: The cold shock protein family*doi://doi.org/10.1016/S0022-2836(02)00259-0

10) Eckert, R. L., Kaartinen, M. T., Nurminskaya, M., Belkin, A. M., Colak, G., Johnson, G. V. W., et al. (2014). Transglutaminase regulation of cell function.*Physiological Reviews, 94*(2), 383-417.

11) Facts and Figures. (n.d.). Retrieved from https://www.alz.org/alzheimers-dementia/facts-figures

12) Fesus, L., & Piacentini, M. (2002). *Transglutaminase 2: An enigmatic enzyme with diverse functions*. England: Elsevier Ltd.

13) Fox, B. A., Yee, V. C., Pedersen, L. C., Trong, I. L., Bishop, P. D., Stenkamp, R. E., et al. (1999). Identification of the calcium binding site and a novel ytterbium site in blood coagulation factor XIII by X-ray crystallography. *Journal of Biological Chemistry, 274*(8), 4917-4923.

14) Ghisaidoobe, A. B. T., & Chung, S. J. (2014). Intrinsic tryptophan fluorescence in the detection and analysis of proteins: A focus on förster resonance energy transfer techniques. *International Journal of Molecular Sciences, 15*(12), 22518-22538.

15) Giráldez-Pérez, R., Antolín-Vallespín, M., Muñoz, M., & Sánchez-Capelo, A. (2014). Models of α-synuclein aggregation in parkinson's disease.*Acta Neuropathologica Communications, 2*(1), 176.

16) Grosso, H., & Mouradian, M. M. *Transglutaminase 2: Biology, relevance to neurodegenerative diseases and therapeutic implications*doi://doi.org/10.1016/j.pharmthera.2011.12.003

17) Gundemir, S., Colak, G., Tucholski, J., & Johnson, G. V. W. (2012). Transglutaminase 2: A molecular swiss army knife. *BBA - Molecular Cell Research, 1823*(2), 406-419.

18) Hohsaka, T., Iijima, I., Abe, R., Kajihara, D., Komiyama, C., & Sisido, M. (2006). FRET analysis of protein conformational change through position-specific incorporation of fluorescent amino acids. *Nature Methods, 3*(11), 923-929.

19) Huang, Y., Zhou, Y., Castiblanco, A., Yang, W., Brown, E. M., & Yang, J. J. (2009). Multiple Ca2+-binding sites in the extracellular domain of the Ca2+-sensing receptor corresponding to cooperative Ca2+Response. *Biochemistry, 48*(2), 388-398.

20) Jang, T., Lee, D., Choi, K., Jeong, E. M., Kim, I., Kim, Y. W., et al. (2014). Crystal structure of transglutaminase 2 with GTP complex and amino acid sequence evidence of evolution of GTP binding site. *PLoS ONE, 9*(9), e107005.

21) Király, R., Csősz, É, Kurtán, T., Antus, S., Szigeti, K., Simon-Vecsei, Z., et al. (2009). Functional significance of five noncanonical Ca2+-binding sites of human transglutaminase 2 characterized by site-directed mutagenesis. *FEBS Journal, 276*(23), 7083-7096.

22) LSPR vs. SPR: What's the Difference? - Nicoya Lifesciences. (n.d.). Retrieved from https://nicoyalife.com/technology/surface-plasmon-resonance/localized-surface-plasmon-resonance-theory/

23) Marques, O., & Outeiro, T. F. (2012). Alpha-synuclein: From secretion to dysfunction and death. *Cell Death and Disease, 3*(7), e350.

24) National Center for Health Statistics. (2018, March 21). Retrieved from https://www.cdc.gov/nchs/pressroom/sosmap/parkinsons_disease_mortality/parkinsons_disease.htm

25) Neurodegenerative Disease Research. (n.d.). Retrieved from http://www.neurodegenerationresearch.eu/

26) Odii, B. O., & Coussons, P. (2014). Biological functionalities of transglutaminase 2 and the possibility of its compensation by other members of the transglutaminase family. *The Scientific World Journal, 2014*, 1-13.

27) Pinkas, D. M., Strop, P., Brunger, A. T., & Khosla, C. (2007). Transglutaminase 2 undergoes a large conformational change upon activation. *PLoS Biology, 5*(12), e327-2796.

28) Reece, K. L., & Moss, R. L. (2007). Removal of contaminating calcium from buffer solutions used in calcium binding assays. *Analytical Biochemistry, 365*(2), 274-276.

29) Sarang, Z., Tóth, B., Balajthy, Z., Köröskényi, K., Garabuczi, É, Fésüs, L., et al. (2009). Some lessons from the tissue transglutaminase knockout mouse. *Amino Acids, 36*(4), 625-631.

30) Seeger, C., Talibov, V. O., & Danielson, U. H. (2017). Biophysical analysis of the dynamics of calmodulin interactions with neurogranin and Ca2+ /calmodulin-dependent kinase II: Biophysical analysis of the dynamics of calmodulin interactions. *Journal of Molecular Recognition, 30*(8), e2621.

31) Sheikh, S., Safia, Haque, E., & Mir, S. S. (2013). Neurodegenerative diseases: Multifactorial conformational diseases and their therapeutic interventions. *Journal of Neurodegenerative Diseases, 2013*, 1-8.

32) Singh, G., Zhang, J., Ma, Y., Cerione, R. A., & Antonyak, M. A. (2016). The different conformational states of tissue transglutaminase have opposing affects on cell viability. *Journal of Biological Chemistry, 291*(17), 9119-9132.

33) Song, M., Hwang, H., Im, C. Y., & Kim, S. (2017). Recent progress in the development of transglutaminase 2 (TGase2) inhibitors. *Journal of Medicinal Chemistry, 60*(2), 554.

34) Steinert, P. M., Nemes, Z., Kee, S., Ahvazi, B., & Kim, H. C. (2002). Three-dimensional structure of the human transglutaminase 3 enzyme: Binding of calcium ions changes structure for activation.*The EMBO Journal, 21*(9), 2055-2067.

35) Ulmer, T. S., Bax, A., Cole, N. B., & Nussbaum, R. L. (2005). Structure and dynamics of micelle-bound human alpha-synuclein. *The Journal of Biological Chemistry, 280*(10), 9595.

36) Viscomi, J. S., Zeczycki, T., & East Carolina University Department of Biochemistry and Molecular Biology. (2016). *Regulation of transglutaminase 2 structure and function by Ca2+ and [alpha]-synuclein*. Greenville, N.C.: East Carolina University. Retrieved from http://eastcarolina.summon.serialssolutions.com/2.0.0/link/0/eLvHCXMwY2AQNtIz0EUrE1CPJWCA3VCHdpqAIeg8On3QPXfMDKygU0FASdY1xAvrRTbgCsBNkIE1FbQrQIiBKTVPhCE0CHKDO9BPCvlpCuDyPh0YhYmgdSXFqQpGCpBjWUuLUhWA9iqAKg-w4qRKBedEI22wYDR4m2usbnFlHuhM4cw8UQZlN9cQZw9dZFfEQ8dX4kEnfBkDkRgDC7DHnirBoGCeaJFsYmFqDjqpxiTJMDXRPMXYMsXSPCnFHNQ8M5VkkMFnkhR-aWkGLmCtDR0HkGFgAXooVRY1hOTAwQYAxC1w5A

37) Wang, C. A., Wang, C. L., Leavis, P. C., Leavis, P. C., Horrocks Jr, W. D., Horrocks Jr, W. D., et al. (1981). Binding of lanthanide ions to troponin C.*Biochemistry, 20*(9), 2439-2444.

38) Wong, C. L., & Olivo, M. (2014). Surface plasmon resonance imaging sensors: A review. *Plasmonics, 9*(4), 809-824. doi:10.1007/s11468-013-9662-3

39) Yasuda, T., Nakata, Y., & Mochizuki, H. (2013). A-synuclein and neuronal cell death. *Molecular Neurobiology, 47*(2), 466-483.

40) Zhou, H., & Pang, X. (2018). Electrostatic interactions in protein structure, folding, binding, and condensation. *Chemical Reviews, 118*(4), 1691-1741.